ANNUAL REVIEWS

Annual Review of Astronomy and Astrophysics

Streams, Substructures, and the Early History of the Milky Way

Amina Helmi

Kapteyn Astronomical Institute, University of Groningen, 9700 AV Groningen, The Netherlands; email: ahelmi@astro.rug.nl

Annu. Rev. Astron. Astrophys. 2020. 58:205–56

The *Annual Review of Astronomy and Astrophysics* is online at astro.annualreviews.org

https://doi.org/10.1146/annurev-astro-032620-021917

Keywords

galaxy formation, galaxy evolution, kinematics and dynamics, thick disk, halo

Abstract

The advent of the second data release of the *Gaia* mission, in combination with data from large spectroscopic surveys, is revolutionizing our understanding of the Galaxy. Thanks to these transformational data sets and the knowledge accumulated thus far, a new, more mature picture of the evolution of the early Milky Way is currently emerging.

- Two of the traditional Galactic components, namely, the stellar halo and the thick disk, appear to be intimately linked: Stars with halo-like kinematics originate in similar proportions from a heated (thick) disk and from a debris from a system named Gaia-Enceladus. Gaia-Enceladus was the last big merger event experienced by the Milky Way and was completed around 10 Gyr ago. The puffed-up stars now present in the halo as a consequence of the merger have thus exposed the existence of a disk component at $z \sim 1.8$. This is likely related to the previously known metal-weak thick disk and may be traceable to metallicities [Fe/H] $\lesssim -4$. As importantly, there is evidence that the merger with Gaia-Enceladus triggered star formation in the early Milky Way, plausibly leading to the appearance of the thick disk as we know it.
- Other merger events have been characterized better, and new ones have been uncovered. These include, for example, the Helmi streams, Sequoia, and Thamnos, which add to the list of those discovered in wide-field photometric surveys, such as the Sagittarius streams. Current knowledge of their progenitors' properties, star formation, and chemical evolutionary histories is still incomplete.

- Debris from different objects shows different degrees of overlap in phase-space. This sometimes confusing situation can be improved by determining membership probabilities via quantitative statistical methods. A task for the next few years will be to use ongoing and planned spectroscopic surveys for chemical labeling and to disentangle events from one another using dimensions other than phase-space, metallicity, or [α/Fe].
- These large surveys will also provide line-of-sight velocities missing for faint stars in *Gaia* releases and more accurate distance determinations for distant objects, which in combination with other surveys could also lead to more accurate age dating. The resulting samples of stars will cover a much wider volume of the Galaxy, allowing, for example, the linking of kinematic substructures found in the inner halo to spatial overdensities in the outer halo.
- All the results obtained so far are in line with the expectations of current cosmological models. Nonetheless, tailored hydrodynamical simulations to reproduce in detail the properties of the merger debris, as well as constrained cosmological simulations of the Milky Way, are needed. Such simulations will undoubtedly unravel more connections between the different Galactic components and their substructures, and will aid in pushing our knowledge of the assembly of the Milky Way to the earliest times.

Contents

1. INTRODUCTION

It is a very exciting time for research on streams and substructures, and their use to shed light on the early history of our own Galaxy, the Milky Way. Although the field now known as

Galactic archaeology has a long history, it is hard to overstate the impact of the second data release (DR2) from the *Gaia* mission (Gaia Collab. et al. 2018b), which took place on April 25, 2018. The combination with data already available from many large spectroscopic surveys, such as APOGEE (Apache Point Observatory Galactic Evolution Experiment; **http://www.sdss.org/dr12/irspec/**) (Majewski et al. 2017), GALAH (Galactic Archaeology with HERMES; **http://www.galah-survey.org/**) (De Silva et al. 2015), RAVE (Radial Velocity Experiment; **http://www.rave-survey.org/project/**) (Kunder et al. 2017), and LAMOST (Large Sky Area Multi-Object Fibre Spectroscopic Telescope; **http://www.lamost.org/**) (Deng et al. 2012), has helped us to obtain a much clearer picture of how the Milky Way and, in particular, its older components have evolved since $z \sim 2$ or, equivalently, 10 Gyr ago.

These new data sets are allowing us to put together, and in a broader context, the many pieces of the puzzle previously reported in the literature to give a much more complete view of the Galaxy's past. The current generation is quite fortunate to be part of this chapter in the history of Galactic astronomy. It is very exciting that we might actually know how and when the Milky Way experienced its last big merger and that it seems likely that this event gave rise to most of the halo near the Sun, which would be predominantly composed of debris from a single object that was accreted about 10 Gyr ago and stars from the heated disk present at the time. This is what *Gaia* has unraveled in conjunction with high-resolution spectroscopic surveys, particularly APOGEE. The rapid progress made in the field since DR2 has been possible thanks to the work of many scientists before DR2, as their work allowed the relatively quick derivation of a rather clear, although not yet fully settled, picture of the sequence of events. This is, in fact, an example of one of the pillars of the scientific enterprise: that we build on previous knowledge. It would have taken much longer to pin down Galactic history to the extent reached thus far had these earlier works not been carried out. *Gaia* DR2, even if only based on data taken during less than half of the mission's nominal lifetime (22 months out of 60), has really helped us to move from a fragmented view to seeing Galactic history in its full glory.

Many excellent reviews have been written over the past 20 years on Galactic archaeology and near-field cosmology, starting with the one by Freeman & Bland-Hawthorn (2002); others include articles by Frebel & Norris (2015) on the first stars and their use for (near-field) cosmology, Bland-Hawthorn & Gerhard (2016) on the structure and dynamics of the Galaxy, and Belokurov (2013) and Johnston (2016) on substructure and tidal debris, as well as the introduction to the Galactic halo by Helmi (2008). An interesting exercise is to read the reviews using the information that we have recently acquired about our Galaxy. The reader is encouraged to put on the new *Gaia* glasses when going through the findings reported in those studies. Hopefully, readers will note that there is much consistency in the results obtained so far, and hopefully these reviews will aid the readers in constructing their own narrative on the basis of the information and hints that we had but did not fully understand at the time.

The first objective of this review is, thus, to present the state of the art in the context of what was previously known about our Galaxy. It should be noted that because we are still in the process of digesting the most recent results from the many ongoing surveys focused on the Milky Way, and because more data will come in the next 5 to 10 years, it is particularly challenging to give an overview that is complete and will stand the test of time. The emphasis and sometimes the interpretation of the recent discoveries reflects the author's own perspective and understanding, while still aiming for an objective and solid account of the facts.

Another objective of this review is to point out new avenues of research now that we have a much better—albeit still sketchy and in a state of flux—understanding of the assembly of the Milky Way. As described in this review, particularly the second half, there are still many small and not-so-small details missing. Solving these will require substantial effort. We will need more detailed

modeling and better hydrodynamical and cosmological simulations. We will have to assemble large, high-resolution spectroscopic data sets with the chemical abundances of millions of stars to be able to pin down their sites of formation and label, as it were, the stars' origin. It should be possible to go back in time even further than 10 Gyr ago, perhaps out to redshift 6–10, by studying stars in the different structures of the Milky Way.

This review starts in Section 2 with a brief description of the different Galactic components following a traditional approach. In Section 3, we move on to Galactic archaeology and discuss the fossils and tools that are available to do this type of work. Then, in Section 4, we dive into one of the components that holds clues to the evolution of the Galaxy at early times, namely, the Galactic stellar halo. We describe the most recent discoveries and how they link to the formation of another ancient component, the thick disk. We focus on this latter component in Section 5. In this journey, we describe not just the data but we also discuss predictions from simulations and models. In Section 6 we describe the next steps, those that would seem to be necessary to really fully unravel how the Milky Way was put together. These as well as the most important conclusions are summarized in Section 7.

2. THE MILKY WAY AND ITS TRADITIONAL COMPONENTS

2.1. Brief Description

The Milky Way is, in general terms, a fairly typical disk galaxy (Bland-Hawthorn & Gerhard 2016). Its estimated stellar mass is $\sim 5 \times 10^{10}\,M_\odot$, which implies a luminosity close to the characteristic value L_* of the galaxy luminosity function. Given its circular velocity of $V_{\rm max} \sim 240$ km s^{-1} (see, e.g., Gravity Collab. et al. 2019), it may be slightly subluminous as it lies a bit below, but within 1σ of, the Tully-Fisher relation.

The Milky Way has several visible components: a thin disk, thick disk, bulge/bar, and stellar halo, as shown in **Figure 1**. Each of these components has individual characteristics. Their stars differ not only in their spatial distributions but, of course, also kinematically, as shown in **Figure 2**. Furthermore, their ages and chemical distributions are also different. This implies that the components are truly physically distinct. Their constituent stars inform us about the various processes that are important in the buildup of a galaxy throughout its life.

We list here a brief description of the main characteristics of the Galactic components:

- The thin disk is the site of ongoing star formation. It is the noteworthiest component of the Galaxy and also gives the Milky Way it its name. Its current star formation rate (SFR) is estimated to be $\sim 1.6\,M_\odot$ year^{-1} (Licquia & Newman 2015), and it seems to have been forming stars for at least 8 or 9 Gyr (Tononi et al. 2019). It is rotationally supported, and most stars move on fairly circular orbits.
- The thick disk is a thicker, more diffuse, and hotter component than the thin disk. Its stars are older than the oldest stars in the thin disk, with estimates using white dwarfs in the Solar vicinity suggesting an age difference of at least ~1.6 Gyr (Kilic et al. 2017). Its metallicity distribution function peaks at a lower metallicity value than the thin disk of [Fe/H] ~ -0.5, and its stars define a separate chemical sequence in, e.g., [α/Fe] versus [Fe/H] space from that defined by the thin disk (Bensby et al. 2003, Fuhrmann 2011), which can be attributed to a different (shorter and more intense) star formation history (see e.g., Chiappini et al. 1997, Haywood et al. 2015). We discuss this in more detail in Section 5.
- The bar/bulge is the most centrally concentrated component, and because it is heavily obscured, our current understanding is somewhat limited, although significant progress has recently been made thanks to new surveys as described in, for example, the reviews by

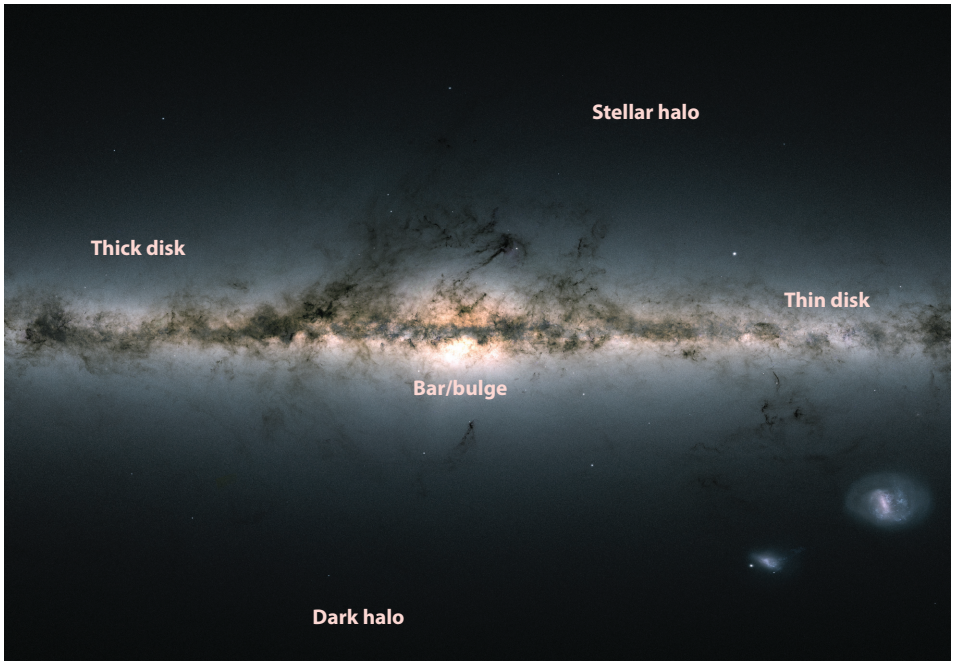

Figure 1

The Milky Way and its various components. This image was obtained using data from the second data release of the *Gaia* mission (Gaia Collab. et al. 2018b). Adapted with permission from *Gaia*/DPAC (Data Processing and Analysis Consortium)/European Space Agency.

Barbuy et al. (2018) and Zoccali (2019). The presence of a classical bulge (i.e., of spherical shape, formed quickly, dispersion supported) is still debated, but its contribution has been constrained by the observed kinematics to be small (<8% of the mass of the disk; Shen et al. 2010). Most of the bulge is in a rotating triaxial structure, the Galactic bar. Estimates of its orientation, pattern speed, and exact extent have undergone revision lately; recent work suggests a rather long bar (Portail et al. 2015, Wegg et al. 2015). Spectroscopic studies show a mix of populations present in the central regions (Ness et al. 2013), some of which are very old (more than 13 Gyr) and metal-rich, with [Fe/H] values up to +0.5 dex, and some of which resemble other Galactic components, such as the thick disk and stellar halo, all of which, of course, peak in terms of their spatial density in the inner Galaxy.

- The stellar halo is the most extended component, but at the same time, it is rather centrally concentrated: The half-light radius traced by the metal-poor globular clusters is ∼0.5 kpc (Bica et al. 2006). It is oblate in the inner regions, with $q \sim 0.6$, and its density is well modeled by a broken power-law (Deason et al. 2011, Xue et al. 2015). The most recent estimates of its total mass yield $\sim 1.3 \times 10^9\,M_\odot$ (Deason et al. 2019, Mackereth & Bovy 2020). The stellar halo contains very metal-poor and old stars. It is discussed in detail in Section 4 of this review.
- The above items refer to the stellar components of the Galaxy, but there is also warm ionized gas in a halo or circumgalactic medium (Richter 2017, Zheng et al. 2019) and cold gas mostly in the disk.

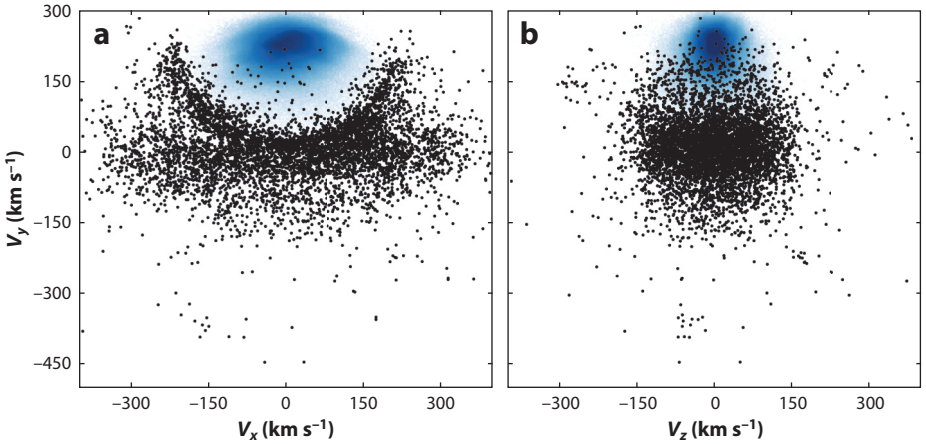

Figure 2

Velocity distribution of stars in the solar neighborhood as determined by *Gaia*. In this figure, all stars from the *Gaia* second data release with full phase-space information, located within 1 kpc of the Sun, and with relatively accurate parallaxes, i.e., with $\varpi/\sigma_\varpi \geq 5$ have been considered. The nearby halo stars are plotted with black dots and defined as those that satisfy $|\mathbf{V} - \mathbf{V}_{\rm LSR}| > 210$ km s^{-1}, for $V_{\rm LSR} = 232$ km s^{-1}, where LSR indicates the local standard of rest. The blue density maps reveal the contribution of the thin and thick disks. The banana-shaped structure seen in the panel *a* reveals an important contribution of hot thick disk–like stars to the halo. Adapted with permission from H.H. Koppelman (see also figure 2 in Koppelman et al. 2018).

If our understanding of gravity is correct, the Galaxy is embedded in a dark matter halo, where most of the mass of the system is located. The characteristics of this halo are not very well constrained. Current estimates of its mass based on *Gaia* DR2 by Posti & Helmi (2019) and Watkins et al. (2019) give $\sim 1.3 \times 10^{12}$ $M_\odot$ (consistent with the range of values quoted by Bland-Hawthorn & Gerhard 2016). Its shape is uncertain and has been the subject of significant debate (Ibata et al. 2001, Helmi 2004, Johnston et al. 2005, Ibata et al. 2013). It is likely slightly oblate in the central regions [Koposov et al. (2010), although Wegg et al. (2019) argue for spherical] and changes to a triaxial shape at large distances (Law & Majewski 2010, Vera-Ciro & Helmi 2013), with the longest axis in the direction perpendicular to the disk (Banerjee & Jog 2011, Vera-Ciro & Helmi 2013, Bowden et al. 2016, Posti & Helmi 2019). The density profile of the dark halo has received less attention thus far (but see Taylor et al. 2016, Eadie & Jurić 2019, Fardal et al. 2019, Yang et al. 2020). An interesting question is the degree of lumpiness of the mass distribution and whether it is consistent with expectations from cold dark matter simulations, which predict a myriad of (dark) satellites (Klypin et al. 1999, Moore et al. 1999, Springel et al. 2008). Recent work on streams is beginning to reveal a complexity that may require the consideration of perturbations by, for example, the Large Magellanic Cloud (Vera-Ciro & Helmi 2013, Erkal et al. 2019, Koposov et al. 2019), as well as a certain amount of smaller scale lumpiness, as suggested by the groundbreaking analyses of Bovy et al. (2017), Price-Whelan & Bonaca (2018), de Boer et al. (2018), Bonaca et al. (2019), and Malhan et al. (2019).

2.2. Link Between the Components and Physical Processes in Galaxy Evolution

The differing characteristics of the various Galactic components suggest each had its own formation path. Nonetheless, it is likely that these paths were interlinked. It should largely be possible

to unravel these formation paths using stars, since these retain memory of their origin. This idea constitutes the pillar of Galactic archaeology, as we discuss in greater detail in Section 3.

The Λ-cold dark matter (ΛCDM) model provides a framework to understand how galaxies form and evolve from first principles (see, e.g., the review by Frenk & White 2012). In this model, galaxies form inside dark matter halos (White & Rees 1978). Most of the dark halos' properties (such as mass function, abundance number, etc.) depend on the characteristics of the cosmological model, including, for example, the power spectrum of density fluctuations, the type of dark matter, and the values of the cosmological parameters (as discussed extensively in Mo et al. 2010). Because in the concordance model there is $\sim 6\times$ more mass in dark matter than in baryons (this is supported by measurements of, e.g., the fluctuations in the cosmic microwave background; Planck Collab. et al. 2016), many of the properties of galaxies, such as how they cluster or their dynamics, are largely dictated by their dark halos. A direct example of this is the process of halo collapse and formation, during which dark halos attract baryonic material from which the (visible components of) galaxies can form. For the baryons in a gaseous configuration to be able to cool and form stars, several conditions need to satisfied (dictated by, e.g., cooling and heating processes and dynamical timescales; see Mo et al. 2010). If these conditions are satisfied, the gas will cool and collapse to the center of their halos while conserving some amount of angular momentum. This results in a gaseous disk that is rotationally supported (Mo et al. 1998), with some amount of random motion depending on the state of the gas (Bournaud et al. 2009). Note that, particularly in the early universe, gas can also be directly accreted as a cold flow and feed the forming galaxy (Dekel et al. 2009). In the cold gas disk, stars will start to form. In fact, most star formation in the Universe takes place quiescently and is not associated with large starbursts (see Brinchmann et al. 2004, Elbaz et al. 2011).

In the ΛCDM model, structure formation proceeds hierarchically via mergers. At early times, mergers were more frequent because of the higher density of the Universe. This means that galaxies were more prone to merge with other galaxies, and hence their disks were more vulnerable. Depending on the mass ratio, such an event could lead to the formation of a bulge (Barnes 1992), or merely to the thickening of the disk (Quinn et al. 1993), and possibly also to the formation of a halo of stars from the original disk and the destroyed satellite (Zolotov et al. 2009, Purcell et al. 2010), as seems to have happened for the Milky Way (see Section 4.2 for details). Depending on the characteristics of the merger, such an event could have also triggered the formation of a bar (Gerin et al. 1990). It is, in fact, likely that the Galactic bar originated from a disk instability. However, it is not clear whether the bar had its origin in the thin disk (Martinez-Valpuesta & Gerhard 2013) or whether the metallicity gradient seen in the bar implies that some of the stars have their origin in the thick disk (see Di Matteo et al. 2015, Fragkoudi et al. 2018, and references therein), as suggested also by their similar chemical abundance patterns (Alves-Brito et al. 2010).

These examples show that there may be strong links between different components of the Milky Way, and that some of their current configurations could be due to or triggered by the same event. On the one hand, these components may share a fraction of their stellar populations, such as the bar and the (primordial) thick disk, or the halo and the primordial thick disk. On the other hand, galaxies at earlier times had higher gas fractions, which could also imply that mergers may have indirectly led to the formation of a significant stellar population in a Galactic component via the triggering of a starburst, as perhaps was the case for the thick disk (see Gallart et al. 2019 and Section 5.2 for more details).

These considerations highlight why we should probably not think of our Galaxy in terms of separate and independent components that have no connection to each other. Rather, we should aim to establish if and how they may be related, given our ultimate goal of unraveling the sequence of events that took place in the history of the Milky Way.

3. GALACTIC ARCHAEOLOGY

3.1. Introduction

Today's commonly used phrase "Galactic archaeology" is often applied to describe research on the formation and history of the Milky Way and its stellar populations. The work of Roman (1950, and several subsequent papers) showing that stars with different chemistry also have different kinematics has been recognized as very influential.[1] The papers by Eggen et al. (1962) and Searle & Zinn (1978), as well as Tinsley (1980) more generally for galaxies, can arguably be considered as pioneering in the field.

In its modern form, the idea behind Galactic archaeology is to use the properties of long-lived stars to reconstruct the Galaxy's history, much in the same way archaeologists use artifacts or rubble to learn about the past. Possibly one of the first printed records of the use of the word "archaeology" in an astronomical context is an article in *The Messenger* by Spite & Spite (1979), where there is a reference to astro-archaeology. In this paper, the authors aim to use old stars to understand the buildup of metals in the universe. The term Galactic archaeology in a more dynamical context is used in the report of IAU Commission 33, "Structure and Dynamics of the Galactic System" (Burton 1988, p. 409), in section 13 (headed by J. Binney):

> Perhaps it is not too fanciful to imagine a field of galactic archaeology opening up, in which painstaking sifting of the contents of each element of phase-space will enable us to piece together a fairly complete picture of how our Galaxy grew to its present grandeur and prosperity.

The turn of the century is approximately the time that the phrase Galactic archaeology was adopted widely by the community, as it begins to appear more frequently in both talks and the printed literature, in part because of the very influential reviews by Bland-Hawthorn & Freeman (2000) and Freeman & Bland-Hawthorn (2002) (see also Bland-Hawthorn 1999, who introduced the term near-field cosmology). Impetus to the field was undoubtedly given by the discovery by Ibata et al. (1994) of the Sagittarius dwarf as direct evidence of an ongoing merger, and subsequently to some extent by discovery of debris streams near the Sun from a past merger in the Hipparcos (**http://sci.esa.int/web/hipparcos/**) data (Perryman et al. 1997) by Helmi et al. (1999).

This time also coincides with the maturing of galaxy formation models (Kauffmann et al. 1993, Baugh et al. 1998, Somerville & Primack 1999) and the establishment of the ΛCDM model as the concordance cosmological model. This allowed significant progress in the theoretical predictions concerning what a galaxy like the Milky Way should have experienced in its lifetime. Thus, Galactic archaeology could also be guided by theory, and some aspects of the cosmological models could now be tested directly from the perspective of the Milky Way. This spirit is particularly evident in the third Stromlo Symposium on the Galactic Halo (Gibson et al. 1999), which took place in Canberra in 1998. For example, the article describing the conference highlights (de Zeeuw & Norris 1999), as well as a quick inspection of the index of the proceedings, will reveal that the theme of accretion and mergers and the use of the fossil record to reconstruct Galactic history were present in many of the participants' contributions to the meeting.

What does Galactic archaeology actually mean? As already mentioned, the idea behind it is that stars have memory of their origin. Low-mass stars live longer than the age of the universe, and hence some will have formed at very early times and have survived until the present day. They will have retained in their atmospheres a fossil record of the environment in which they were

[1]The reader may wish to consult the prefatory chapter of the 2019 volume of the *Annual Review of Astronomy and Astrophysics* (Roman 2019) or listen to the associated podcast of J. Bland-Hawthorn interviewing N.G. Roman a few months before her passing away in 2018.

born. This is because the chemical composition of a star's atmosphere, particularly if it has not yet evolved off the main sequence, reflects the chemical composition of the interstellar medium (ISM) (the molecular cloud) in which it formed. This means access to the physical conditions present at the time of formation of the star. For very old stars, the conditions might have been very different than today (leading, for example, to different initial mass functions), and therefore, such stars provide us with a window into the early Universe (Frebel & Norris 2015). Stars with similar chemical abundance patterns likely have a common origin. This common DNA, so to speak, would then allow the identification of stars with similar histories; this is known as chemical tagging. The foundations of this approach were put forward by Freeman & Bland-Hawthorn (2002) and are briefly discussed in Section 3.2.

Another particularly useful way to track Galactic history is through precise measurements of stellar ages. Knowing the ages of stars would permit us to date the sequence of events that led to the formation of the different components of the Galaxy. However, obtaining precise ages for very old stars is very difficult. Even 10% errors at 10 Gyr imply going from redshift 1.8 to 2.3, and a difference of only 2 Gyr exists for a star born at redshift 2 versus redshift 6. Nonetheless, the combination of ages and chemical abundances of stars is very powerful and can be used to establish a timeline (i.e., in a closed system, stars born later will be more metal-rich).

Stars also retain memory of their origin in the way they move. For example, as a galaxy gets torn apart by the tidal forces of a larger system like the Milky Way, the stripped stars continue to follow similar trajectories as their progenitor system (Johnston et al. 1996, Johnston 1998). This implies that if the Milky Way halo is the result of the mergers of many different objects, their stars should define streams that crisscross the whole Galaxy (Helmi & White 1999). As becomes clear in Section 3.3, access to full phase-space information is critical to reconstructing the past history of the Galaxy using dynamics.

3.2. Astrophysical Properties of Stars: Chemical Abundances and Ages as a Tool

As briefly discussed above, the ages and chemical abundances of stars are two of the tools used in Galactic archaeology.

3.2.1. Chemical abundances. The discovery that stars with different metallicities (or iron abundances) have different chemical abundance patterns was first hinted at the end of the 1960s (Conti et al. 1967), and one of the first systematic studies of metal-poor stars is the work of Sneden et al. (1979), interpreted in the context of supernovae (SNe) type I and II and Galactic nucleosynthesis models.

The reason for the variety of chemical elemental abundance patterns is that different elements are produced in different environments and on a range of timescales (McWilliam 1997). For example, α elements such as O, Mg, Si, Ca, S, and Ti are released in large amounts during the explosion of a massive star as an SN, an event that occurs only a few million years after the star's birth. Iron-peak elements are also produced in type Ia SNe, which are the result of a thermonuclear explosion of a white dwarf in a binary system, although the details of the burning, the number of white dwarfs involved, and their masses are under debate (see, e.g., the review Maoz et al. 2014). Because both stars in the binary are of lower mass, these SN explosions take place typically on a longer timescale than for type II SNe, of the order of 0.1 to a few Gyr (e.g., Matteucci & Recchi 2001). In terms of the chemical evolution of a (closed) system, we thus expect that [α/Fe] will eventually decrease as time goes by as the ISM of the system becomes polluted by type Ia SNe. When a significant number of such explosions has occurred, the initial nearly constant [α/Fe] trend with

[Fe/H] bends over, and this leads to the appearance of a knee, after which [α/Fe] can only decrease further (unless there is some fresh gas infall).

Heavier elements beyond the iron peak are created by neutron capture processes, through the so-called slow (s) and rapid (r) processes. When the neutron flux is relatively low, i.e., the timescale between neutron captures is large compared with that of the β-decay, the s-process can occur. This can take place, for example, in the envelopes of asymptotic giant branch (AGB) stars (Busso et al. 1999), and the contribution of low-mass AGB stars (1–3 $M_\odot$) appears to be particularly important in the chemical history of the Galaxy (see e.g., Bisterzo et al. 2010, and references therein; also Battistini & Bensby 2016). For low metallicities (at early times), however, stars with such masses will not have not had enough time to reach the AGB phase to be significant contributors of these elements (see Travaglio et al. 2004, and for a comprehensive review on s-process elements, see also Käppeler et al. 2011). A prime example of an element for which the s-process is dominant at [Fe/H] $\gtrsim -1.5$ is Ba (Arlandini et al. 1999).

The r-process, in contrast, occurs when the neutron flux is sufficiently high to allow for rapid neutron captures. This could occur in type II SN environments, for example, but also in the mergers of two neutron stars and of neutron stars with black holes, or in magneto-rotational SNe (as explored, for example, in the Galactic simulations of Haynes & Kobayashi 2019). The recent discovery of Sr in the spectra of the kilonova following the gravitational-wave event GW170817 (Watson et al. 2019) clearly demonstrates that the r-process does occur in neutron star mergers. Nonetheless, the exact sites and conditions under which the various neutron-capture elements are produced, particularly at very low metallicities, have not yet been fully settled, and there may be different channels for producing them [see the excellent review by Sneden et al. (2008) and the more recent extensive review by Cowan et al. (2019)]. Besides Sr, a very typical r-process element is Eu, while, for example, Nd is produced almost equally by the r- and s-processes at the solar metallicity (Arlandini et al. 1999).

The information that can be obtained from detailed chemical abundance analysis underpins the principle of chemical tagging, as put forward by Freeman & Bland-Hawthorn (2002). The chemical DNA of stars born in a variety of environments will be different (De Silva et al. 2015). Although in principle each molecular cloud will have its own chemical composition, and this is likely to differ from cloud to cloud in a galaxy, in practice the differences for clouds collapsing at the present day may be small, making it very difficult to disentangle (relatively young) groups of stars of common origin on the basis of their chemistry alone, unless extremely accurate measurements of many different elements are available (although not impossible; see, e.g., De Silva et al. 2006). It would be very interesting to associate each star in a galaxy to its parent molecular cloud because this would potentially reveal the physical processes acting on 1–100-pc scales, i.e., the regime of the interplay between dynamics, star formation, and stellar feedback. Yet this is very challenging, and thus, a less demanding form of chemical tagging, known as weak tagging or chemical labeling,[2] has been put forward. With chemical labeling, we study different (larger) regions or components in the Galaxy to unravel, for example, migration mechanisms in the disk(s) (Minchev et al. 2017, Ness et al. 2019). This allows us to establish whether a star that is now part of the thick disk actually formed in the thin disk in the inner Galaxy and migrated to the Solar vicinity (Schönrich & Binney 2009).

In the context of the halo, the underlying thought behind chemical labeling is that stars born in different systems (accreted galaxies or in the proto–Milky Way) follow their own distinct chemical sequences because each system had its own particular star formation and chemical enrichment history. This is, in fact, what we see for stars associated with the different dwarf galaxies in the

[2]This last term was coined by Vanessa Hill, possibly in the year 2010.

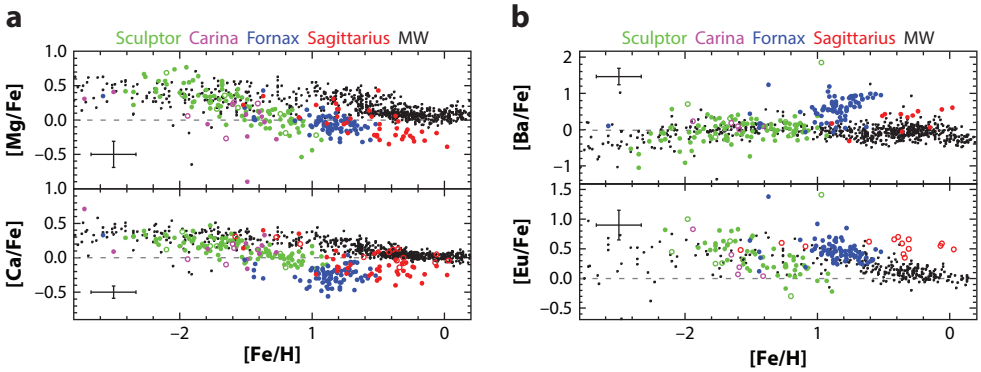

Figure 3

Chemical abundances of stars in four dwarf spheroidal galaxies (*colors*) and the Milky Way (*black*). Panel *a* shows the behavior with [Fe/H] of two α elements, Ca and Mg, while panel *b* shows the trends followed by Ba (an s-process element at [Fe/H] $\gtrsim -1.5$ or thereabouts) and Eu (r-process) with metallicity. Adapted with permission from Tolstoy et al. (2009).

Local Group, as shown in **Figure 3**. Notice also how the sequences followed by the stars in the different galaxies appear to be sorted according to the mass of the system. In particular, the trend of [α/Fe] with [Fe/H] could be an interesting discriminator of stars born in accreted dwarf galaxies. Low-mass galaxies that have only formed one generation of stars will likely only have high [α/Fe] at low [Fe/H], while galaxies that have managed to sustain star formation longer might have very low [α/Fe] even at low [Fe/H] because of inherently inefficient star formation, and hence their debris may be more easily identifiable.

Other potentially promising chemical labels for the identification of stars born in accreted dwarf galaxies appear to be r-process element abundances (see, e.g., Xing et al. 2019). In the Galactic halo, there is a large scatter in [r-process/Fe] at low metallicity (as seen, to some extent, in **Figure 3*d***), which could indicate a range of birthplaces. While most ultrafaint dwarf galaxies appear to be deficient in r-process elements, the Reticulum II galaxy contains proportionally many r-process–enhanced stars (~78%, compared with less than 5% in the Galactic halo; Ji et al. 2016). The way to understand this is that the events leading to the formation of r-process elements are so rare that they have not occurred in most ultrafaint dwarfs (given their low masses). But if one event does happen, it immediately enriches the entire galaxy. Thus, stars with extreme r-process abundances could have their origin in such galaxies (Brauer et al. 2019). For more massive galaxies, clustering in r-process elemental abundances might be expected (Tsujimoto et al. 2017), which, combined with the behavior of [α/Fe] or [Fe/H], could enhance their utility for chemical labeling (Skúladóttir et al. 2019).

Chemical labeling has also been used to identify field halo stars that may have originated in disrupted globular clusters (Martell et al. 2016, Fernández-Trincado et al. 2019). Searches for these stars make use of peculiarities in the abundance patterns such as, for example, anticorrelations in [Na/O] (Carretta et al. 2009), or more generally, depletions in, e.g., C, O, and Mg, and enhancements in N, Na, Al, and Si (see Gratton et al. 2019 and references therein).

3.2.2. Ages. In comparison with chemical abundance estimation, the determination of precise ages, particularly for old stars, is much more difficult. Age determination has traditionally been done via isochrone fitting. Recently, Bayesian inference tools have been employed to derive ages for large numbers of stars by using not only multicolor photometry but also astrometric data

from *Gaia* and chemical abundance information provided by large spectroscopic surveys (see, e.g., Queiroz et al. 2018, Sanders & Das 2018, and also Mints & Hekker 2018). Such ages tend to be more reliable, particularly in comparison with those based only on photometry.

Recently, a new way of estimating ages using information about the internal structure of a star (other than the Sun) has become possible via asteroseismology. This quickly growing field is providing new insights and understanding on stellar evolution and, as a consequence, on age determination (Michel et al. 2008, Chaplin et al. 2014). Asteroseismology uses time series of photometry of outstanding quality with campaigns that may take several months or years depending on the type of star [main sequence, red giant branch (RGB), or AGB]. The photometric variations are due to internal oscillations, and their frequencies depend on the star's mass, radius, and effective temperature. Because the frequencies relate in different ways to each of these parameters, the mass of a star can, in principle, be derived with knowledge of the basic frequencies as well as of its temperature from, for example, broad-band photometry. The star's mass can then be used to determine its age using stellar evolution models (Chaplin & Miglio 2013, Miglio et al. 2013).

In the recent past, CoRoT (*Convection, Rotation and Planetary Transits*; **http://sci.esa.int/corot/**) (Auvergne et al. 2009) and *Kepler* (**https://www.nasa.gov/mission_pages/kepler/overview/index.html**) (Gilliland et al. 2010) have been providing new gold standards that allow for better age determination from the frequencies of oscillations of the stars. By calibrating on these, it is possible to obtain independent constraints on, e.g., the gravity of a star ($\log g$), which can then be used as a prior for the analysis of spectroscopic surveys. This then results in a larger sample of stars that have been (indirectly) calibrated, and translates into more accurate stellar parameters determinations, which in combination with isochrone fitting can then yield ages for large samples of stars (see, e.g., Valentini et al. 2017). The recently launched TESS (*Transiting Exoplanet Survey Satellite*; **https://tess.mit.edu/**) (Ricker et al. 2015) and the upcoming PLATO (*Planetary Transits and Oscillations of Stars*; **http://sci.esa.int/plato/**) mission (Rauer et al. 2016) will monitor and characterize large samples of stars, for which ages will then be readily available—plausibly much more accurately than has ever been possible until now, as argued by Kollmeier et al. (2019).

3.3. Kinematical Properties of Stars: Dynamics as a Tool

As mentioned earlier, when a galaxy is disrupted by tidal forces, its stars continue to follow closely the trajectory of the system they used to belong to. A regular orbit (a trajectory), may be characterized by the integrals of motion (IoM), such as energy E, total angular momentum (for a spherical system) or one of its components (in the case of an axisymmetric galaxy, L_z), or by the associated actions, such as J_R, J_ϕ, and J_z for an axisymmetric system (Binney & Tremaine 2008). Since a small galaxy may be seen as an ensemble of stars with similar positions and velocities, this implies that their IoM (or their orbits) are also similar. Hence, if these are conserved through time (as is expected to hold, to first order, for a collisionless system such as a galaxy), this implies that the tidally stripped stars will follow very similar orbits to their progenitor. This results in the formation of a stream (Helmi & White 1999). A stream may thus be seen as a portion of an orbit populated by stars (to first order; see Sanders & Binney 2013 for caveats). This explains why streams are long and narrow if they originated from a small system or formed recently [for more information, see the excellent review by Johnston (2016)].

In the case of a more massive object, tides act in the same way, but the stars that are stripped at any given point in time have a larger range of values of the integrals (i.e., of energies), which results in a broader population of orbits and hence in broader streams (that are sometimes hard to distinguish spatially). The process is not different from that affecting less massive objects, but the end product has a different visual appearance and higher complexity, particularly if the parent

object is disky, in which case sharper and asymmetric tails may arise depending on the details of the configuration of the merger (Quinn 1984; see also Toomre & Toomre 1972, Eneev et al. 1973). Furthermore, the morphological features of the debris also depend on the type of orbit of the system (Hendel & Johnston 2015, Amorisco 2017). For example, if the orbit of the progenitor was fairly radial, then shells are very pronounced. These correspond to the turning points of the orbits of the stars (Helmi & White 1999, Tremaine 1999). If the orbit was circular, then there are no turning points, and hence no shells. An example of the spatial evolution of debris on a somewhat radial orbit (with apocenter/pericenter ≈4.5) is shown in the top panels of **Figure 4**.

The properties of a stream depend on the extent of the parent object, the time since it formed (i.e., since a star became unbound) t, and the characteristic orbital timescales, which we denote as $t_{\rm orb}$. For a dispersion-supported progenitor, the density of a stream at a given point in space may be roughly expressed as $\rho \propto (t_{\rm orb}/t)^3 \times 1/(R\sigma^2)$ (for details and the full derivation, see Helmi & White 1999). Here, R and σ are the characteristic size and velocity dispersion of the progenitor system. The dependence on time t is related to the form of the potential and the number of independent orbital frequencies (see Vogelsberger et al. 2008). Here, it is assumed to be axisymmetric and the orbit to be quasi-regular (and nonresonant), hence the dependence on t^{-3}. The expression shows that in the first stages of the dispersal ($t \sim t_{\rm orb}$), the debris has a high density and therefore remains spatially coherent, leading to easily detectable overdensities on the sky, such as those discovered in the Sloan Digital Sky Survey (SDSS; **https://www.sdss.org/**) by Belokurov et al. (2006). This is typically the regime of streams orbiting in the outer halo, since $t_{\rm orb}$ there is large and the tidal forces are less strong, implying also that t is small. For the inner halo, however, the orbital timescales are short; therefore the density will decrease quickly, even for streams originating in small objects.

The behavior of stars in a stream is different if their orbits are irregular or chaotic. In that case, the rate of divergence will no longer be a power law but exponential, and phase-mixing is therefore much faster (see Price-Whelan et al. 2016). In contrast, if the orbit is resonant, stars take longer to spread out, and the debris can remain spatially coherent over more extended timescales.

As time goes by, debris streams mix spatially, i.e., they become long enough that they may cross each other, and therefore a single system can be responsible for multiple streams in a given location in the Galaxy. What characterizes each of the streams is that locally, the stars have very similar velocities (in this sense, the stars are truly streaming through the host galaxy). Furthermore, because of the conservation of phase-space density (or volume), as a stream becomes longer and longer, its velocity dispersion will have to decrease, i.e., $\Delta^6 w \sim \Delta^3 x \Delta^3 v$, and since $\Delta^3 x$ (the spatial extent covered by the debris, or $1/\rho$) grows in time, this means that $\Delta^3 v$ decreases with time locally, as shown by Helmi & White (1999) (and see Buckley et al. 2019 for a slightly different and interesting application of these concepts). This implies that a given location in the Galaxy may have many different moving groups sharing a common origin, as is clearly apparent in **Figure 4*f***, which depicts a phase-space slice of stars in a simulation of a relatively massive accreted satellite.

From these considerations, it transpires that to detect each of the predicted moving groups, large samples of stars with accurate kinematics are needed. Helmi & White (1999) estimated analytically (this was later confirmed using cosmological simulations by Helmi et al. 2003, Gómez et al. 2013) that if the whole stellar halo had been built via mergers, approximately 500 streams would be expected in the halo near the Sun (independently of whether 10 or 100 galaxies had been accreted). Given that the velocity dispersion of the halo is ∼100 km s^{-1}, the velocity resolution required would be $100/\ (500)^{1/3} \sim 13$ km s^{-1}, and the sample size needed would have to contain at least as many as 5,000 halo stars to yield, on average, 10 stars per stream. These estimates have nearly been met by *Gaia* DR2. Of course, higher precision and larger numbers of tracers would be necessary to go beyond the simple detection of granularity (Gould 2003) to the full characterization of the streams and their parent objects.

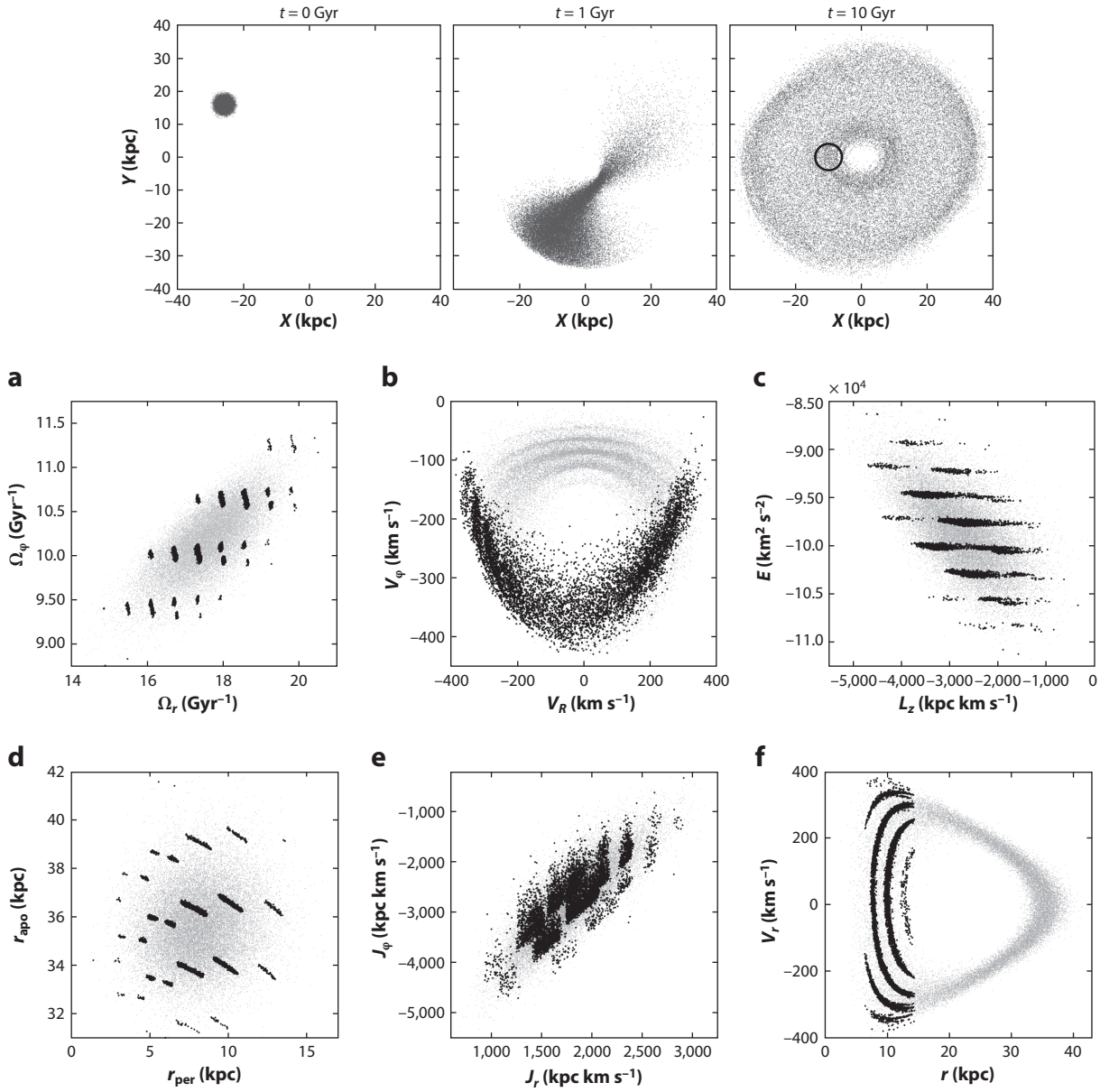

Figure 4

Comparison of various spaces commonly used to identify merger debris: (*a*) frequency space, (*b*) velocity space, (*c*) energy and L_z, (*d*) orbital pericenter versus apocenter, (*e*) actions space, and (*f*) phase-space slice of r versus V_r. The accreted satellite depicted here was evolved in a spherical Plummer potential (of mass 10^{12} $M_\odot$ and $b \sim 22$ kpc) for 10 Gyr. It was non-self-gravitating, spherical, and represented with a 6D Gaussian with $\sigma_x \sim 1$ kpc and $\sigma_v = 22$ km s^{-1}. These characteristics make it comparable to the dwarf elliptical galaxy NGC 185, whose luminosity is only a factor of a few lower than that of the whole Galactic stellar halo. As a result of this large initial extent, the debris occupies a large volume in phase-space. The top panels show X-Y distribution at three different times. The black circle indicates the location of a Solar neighborhood sphere of 4-kpc radius. In panels *a–f*, the gray dots show all satellite particles, and the black dots represent those inside the sphere, revealing the presence of multiple streams in the system. Adapted with permission from figures 4 and 5 of Gómez & Helmi (2010).

As described above, debris originating in a single galaxy is thus expected to have similar IoM (which include, of course, the adiabatic invariants). This has led to the search for ancient accretion events by looking for lumpiness in a space of IoM. The first application of this method was by Helmi et al. (1999), which led to the discovery of the Helmi streams. Then, a proof of concept of what would be possible with a mission like *Gaia* was given by Helmi & de Zeeuw (2000). Diagrams of E versus L_z or L_z versus $L_\perp$ (where $L_\perp^2 = L^2 - L_z^2$ acts as a proxy for a third integral) are now widely used to establish Galactic accretion history. The advantage of using IoM is that all the individual streams (or wraps) of a single object fold into defining a single clump (compare for example, the ensemble of gray points in **Figure 4*c*,*e*** to **Figure 4*b***). Therefore, the precision required on the measurements is less demanding and the signal of a clump in IoM is higher, because the number of stars in a clump is the total number of stars from each of the streams from a given object added together.

There are two caveats, however. In an ideal case, energy or other IoM would be conserved. However, the gravitational potential in which the streams have evolved must have changed with time, implying that this is not exactly true. Nonetheless, Gómez et al. (2013) and Simpson et al. (2019), for example, have shown that substructure is still present in these spaces, even in simulations of the full hierarchical assembly of the halo. Actions, being adiabatic invariants, are better conserved, although more difficult to compute (but see Sanders & Binney 2016). Thus far, however, there has not been a real need to resort to them for the identification of merger debris. The likely reason is that the volumes probed so far by data with full phase-space information (6D) are sufficiently small that in the expression $E = 1/2v^2 + \Phi(\mathbf{x})$, the potential term is approximately constant, i.e., $\Phi(\mathbf{x}_{sun}) = \Phi_0$, and so time variation, or even limited knowledge of the exact form of the potential, has not been a limiting factor. The situation will change as we begin to explore beyond the solar neighborhood, especially with *Gaia* DR3 and subsequent *Gaia* data releases.

Only if all the stars from a given accreted system were mapped would the defined clump be fully smooth (in the absence of dynamical friction). As discussed above, when we observe locally, we typically only probe portions of debris streams. This implies that we expect substructure to be present within a clump associated with a given object in IoM space when using spatially localized samples of stars. This is clearly seen in **Figure 4*c***, where the gray particles denote all the stars from the system (independent of their final location within the host) and those in black indicate the stars inside the small volume indicated by the circle in the top right panel of **Figure 4**. Substructure in IoM may also appear if the system is very massive and thus suffered dynamical friction. In that case, the orbit will have changed with time, and material lost early can be on significantly different orbits than that lost later.

Individual streams or portions of streams are particularly apparent in frequency space, as can be seen in **Figure 4*a***. This is because the individual streams each have their own characteristic frequency (which defines their phase along the orbit; see McMillan & Binney 2008, Gómez & Helmi 2010). The regular pattern seen in **Figure 4*a*** depends on the time of accretion of the system since $\Delta\Theta = \Delta\Omega t$, where $\Delta\Theta$ represents the difference in phase and $\Delta\Omega$ is the separation between neighboring clumps, i.e., a characteristic scale in frequency space. Therefore, since the stars plotted in this figure all have roughly the same location but differ in phase by $\Delta\Theta \sim 2\pi n$ (with n an integer), this implies that t could be inferred by applying a Fourier analysis, provided enough stars are found in each stream (Gómez & Helmi 2010). It turns out that frequency space is also useful for constraining the mass growth or time variation of the gravitational potential as the characteristic regular pattern becomes distorted depending on how the system has evolved (Buist & Helmi 2015, 2017). It may be possible to measure these effects using samples of nearby main sequence halo stars, as these stars are numerous and their velocities and distance estimates may be more accurate because of their relative proximity.

4. THE GALACTIC HALO

4.1. Generalities

Mergers play a key role in the hierarchical cosmological paradigm. This is, after all, by and large the way that galaxies build up their dynamical mass, i.e., their dark halos (Wang et al. 2011). Therefore, tracking mergers is very important toward the goal of unraveling the buildup of Galactic systems. The only way we have to track past mergers over long timescales is by resorting to stars.

This is why the stellar halo of the Galaxy could be considered the prime component to disentangle the merger history of the Galaxy. This is where disrupted galaxies, cannibalized by the Milky Way, most likely have deposited their debris. Some debris may be deposited in the thick disk by satellites on low-inclination orbits (Abadi et al. 2003). It is also a place where we may find heated stars from the disk, i.e., from those present at the time of the mergers that were perturbed on to hotter orbits (Zolotov et al. 2009, Tissera et al. 2013). Most of the mass in the inner regions of Milky Way–like dark halos is predicted to originate in a few massive progenitors (Helmi et al. 2002, Wang et al. 2011), implying that these have hosted sizable luminous galaxies (Cooper et al. 2010). Therefore, most of the information regarding these mergers will be traceable in the stellar halo.

The stellar halo is interesting not only from the point of view of the merger history, but also, as mentioned earlier, because it contains some of the oldest stars and the most metal-poor ones (possibly together with the bulge). This is not necessarily a coincidence. The existence of a mass-metallicity relation for galaxies implies that the proto–Milky Way was generally the most massive object in its cosmic neighborhood. This implies that accreted galaxies were less massive than the proto–Milky Way and hence, on average, more metal-poor than the disk. Since these objects deposit debris in the stellar halo, it will naturally have a lower metallicity. (Of course, this shifts the question to understanding why and how such a mass-metallicity relation arises; see, e.g., Tremonti et al. 2004). Since there is also a correlation between mass and SFR, even though the first stars to form in the Galaxy might have been very metal-poor (or population III), the ISM of the protogalaxy was likely quickly enriched because of its high SFR, reaching a higher overall metallicity, as observed, for example, in the Galactic bulge/bar region (see, e.g., Matteucci et al. 2018).

Understanding the age distribution is trickier because there are fewer precise constraints. However, there is a simple explanation for why the halo should generally be older than the thin disk. Since mergers were much more frequent in the past, a thin disk could only grow to its full current extent after the major epoch of merger activity. The concordance model predicts that the first stars will form in the highest density peaks, which will collapse first and which are typically associated with the more massive objects at later times (e.g., Diemand et al. 2005). This would mean that the first stars in our cosmic environments ought to have formed in the proto–Milky Way. Cosmological simulations suggest these first stars are likely part of the bulge or inner spheroid (White & Springel 2000, Tumlinson 2010, Starkenburg et al. 2017, El-Badry et al. 2018), whereas the outer halo is slightly younger. Thus, a slight age gradient (recall that we are discussing the epoch before the thin disk as we know it was in place) could arise from the fact that lower-mass objects typically form their first stars a bit later. Later accreted objects would also have continued forming stars longer and so contributed to the trend (Carollo et al. 2018). An age gradient was what Searle & Zinn (1978) discovered when studying the age distribution of halo globular clusters, and what led to their fragments model of the formation of the halo. Outer globular clusters are younger, and this is also apparent in recent studies of blue horizontal branch stars (Santucci et al. 2015). However, the age and metallicity distributions, particularly of the outer halo, could be rather patchy and could depend on the specifics of the merger history (e.g., orbits, time of infall) and mass spectrum of accreted objects (e.g., Font et al. 2006).

In summary, because the stellar halo contains proportionally more pristine stars, it gives us a window into the physical conditions present in the early universe (e.g., Frebel & Norris 2015) and also on the early phases of the assembly of the Milky Way, hence its relevance in a cosmological context.

4.2. State of the Art/Most Recent Discoveries

Our knowledge of the Galactic halo has increased greatly in the past 20 years. Relatively deep wide-field photometric surveys such as SDSS (York et al. 2000), Pan-STARRS (the Panoramic Survey Telescope and Rapid Response System; **https://panstarrs.stsci.edu/**) (Chambers et al. 2016), and more recently DES (the Dark Energy Survey; **https://www.darkenergysurvey.org/**) (Abbott et al. 2018), have revealed large overdensities on the sky and many narrow streams (Bernard et al. 2016, Shipp et al. 2018). These are direct testimony of accretion events that have built up the outer halo, as discussed in the reviews by Belokurov (2013) and Grillmair & Carlin (2016), as well as other articles in the book edited by Newberg & Carlin (2016).

Gaia DR2 is, meanwhile, currently driving a true revolution in our understanding of the inner Galactic halo. This might have been expected because of the need for full phase-space coordinates for large samples of stars to pin down formation history (discussed in Section 3.3). More unexpected, perhaps, was the discovery that a large fraction of the halo near the Sun appears to be constituted by the debris from a single object, named Gaia-Enceladus (Helmi et al. 2018). This object is sometimes referred to as Gaia Sausage because of its kinematic signature (Belokurov et al. 2018, Deason et al. 2018). The other very important contributor in the vicinity of the Sun to stars on halo-like orbits is the (tail of the) Milky Way thick disk (Gaia Collab. et al. 2018a, Haywood et al. 2018, Koppelman et al. 2018), as can be seen **Figure 2*a***. These (proto–)thick disk stars were likely dynamically heated during the merger with Gaia-Enceladus (Helmi et al. 2018, Di Matteo et al. 2019). We elaborate on these points below.

4.2.1. Gaia-Enceladus. Although the presence of stars with metallicities typical of the thick disk but with halo-like kinematics had been reported before *Gaia* DR2 (most recently by, e.g., Bonaca et al. 2017), the distinction in the kinematics had not been so clearly seen until DR2, as can be appreciated from the comparison between **Figure 5*a*** and ***b***, and by inspection of **Figure 6** compared with **Figure 2*a***. For stars within 2.5 kpc of the Sun and with $|\mathbf{V} - \mathbf{V}_{\rm LSR}| > 200$ km s^{-1}, i.e., traditionally the regime of the halo, approximately 44% of the stars are in the hot thick disk region ($200 < |\mathbf{V} - \mathbf{V}_{\rm LSR}| < 250$ km s^{-1}), while a large fraction of those remaining (between 60% and 80% depending on the exact definition) are in the elongated structure that is due to Gaia-Enceladus and indicated **Figure 5*b*** (see Koppelman et al. 2018). Similar percentages have been reported by, e.g., Bonaca et al. (2017), Di Matteo et al. (2019), and Belokurov et al. (2020).

These findings link to what was arguably one of the first stunning surprises on the halo in *Gaia* DR2: The color-(absolute) magnitude diagram of stars with halo-like kinematics (i.e., selected to have tangential velocities $V_{\rm T} \gtrsim 200$ km s^{-1}) presented by the Gaia Collaboration (Gaia Collab. et al. 2018a) revealed the presence of two clearly distinct sequences, as shown in the top row of **Figure 7**. These well-defined sequences point to the presence of distinct stellar populations (i.e., with different ages and metallicities) and are evocative of a dual halo (see Carollo et al. 2007, and discussed in some detail in Section 4.2.2). The authors (Gaia Collab. et al. 2018a) tentatively suggested that the older and more metal-poor sequence corresponded to low α-abundance stars on retrograde orbits first reported by Nissen & Schuster (2010, 2011). Then Koppelman et al. (2018) demonstrated that this sequence was dominated by the large kinematic structure (or blob, as it was referred to by the authors), seen in **Figure 5*b***.

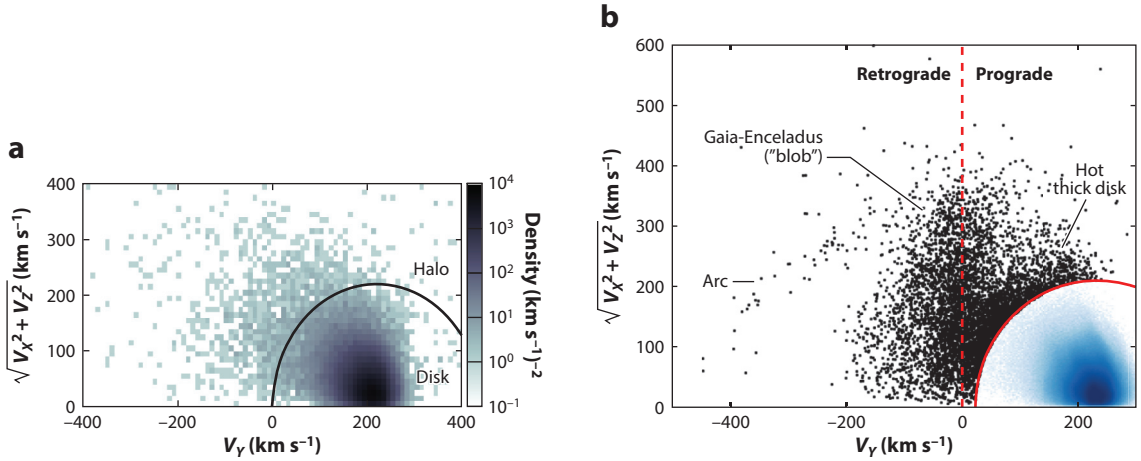

Figure 5

Toomre diagram for nearby stars before (*a*) and after (*b*) *Gaia* second data release (DR2). Panel *a* shows the state of the art before DR2, constructed by Bonaca et al. (2017) using proper motions from the Tycho-Gaia astrometric solution (released with *Gaia* DR1; Gaia Collab. et al. 2016, Lindegren et al. 2016) and line-of-sight velocities and distances from RAVE (the Radial Velocity Experiment survey) (Casey et al. 2017, Kunder et al. 2017). Panel *b* shows the diagram published in Koppelman et al. (2018) using DR2 data. The disjoint kinematic natures of the blob and the hot thick disk are unmistakably apparent in this figure. Figure adapted from Koppelman et al. (2018), and reproduced with permission from the American Astronomical Society.

Driven by these findings, and by the fact that the mean motion of the stars in the kinematic structure was slightly retrograde (as appreciated from the location of the red vertical line **Figure 5*b***), Helmi et al. (2018) selected these stars and showed that they define a well-populated extended chemical sequence of at least 1 dex in [Fe/H] that runs below that of the thick disk in [α/Fe] versus [Fe/H], as seen in **Figure 7*b***. Because the stars in question have lower [α/Fe] at the [Fe/H] where there is overlap with thick disk (which, by and large, must have formed in-situ), this immediately implies that the stars formed in a different system than the thick disk, as [α/Fe] will generally decrease as [Fe/H] increases. This means that these stars must have been accreted. Furthermore, because the majority of the stars in the nearby halo are part of the blob (if they are not in the tail of the thick disk), this implies that a large fraction of the halo near the Sun has been accreted. The accreted system is what has been called Gaia-Enceladus (see the sidebar titled Gaia-Enceladus/Gaia Sausage).

The presence of a significant α-poor (low Mg) chemical sequence was first reported by Hayes et al. (2018), who used data from the APOGEE survey. It was, however, hard for the authors to determine which component the stars in this sequence belonged to because of the lack of proper motion information (their study was carried out just a few months before *Gaia* DR2) or the magnitude of this population. Nonetheless, from the line-of-sight velocities, Hayes et al. (2018) concluded that the stars had halo-like kinematics and that because of the characteristics of the sequence, they likely represented an accreted population. These considerations led Fernández-Alvar et al. (2018) to fit a chemical evolution model. These authors showed that the sequence could be reproduced if the stars had formed in a system with an average SFR of 0.3 $M_\odot$ year^{-1} over a period of 2 Gyr or so. By integrating this SFR, Helmi et al. (2018) subsequently estimated a stellar mass of $\sim 6 \times 10^8\, M_\odot$ for Gaia-Enceladus. Since the existence of a sequence had been known about for some years (since Nissen & Schuster 2010), studies had already compared the ages of the stars in the sequence to those in the thick disk sequence in the metallicity range $-1 \lesssim$ [Fe/H] $\lesssim -0.6$ (Schuster

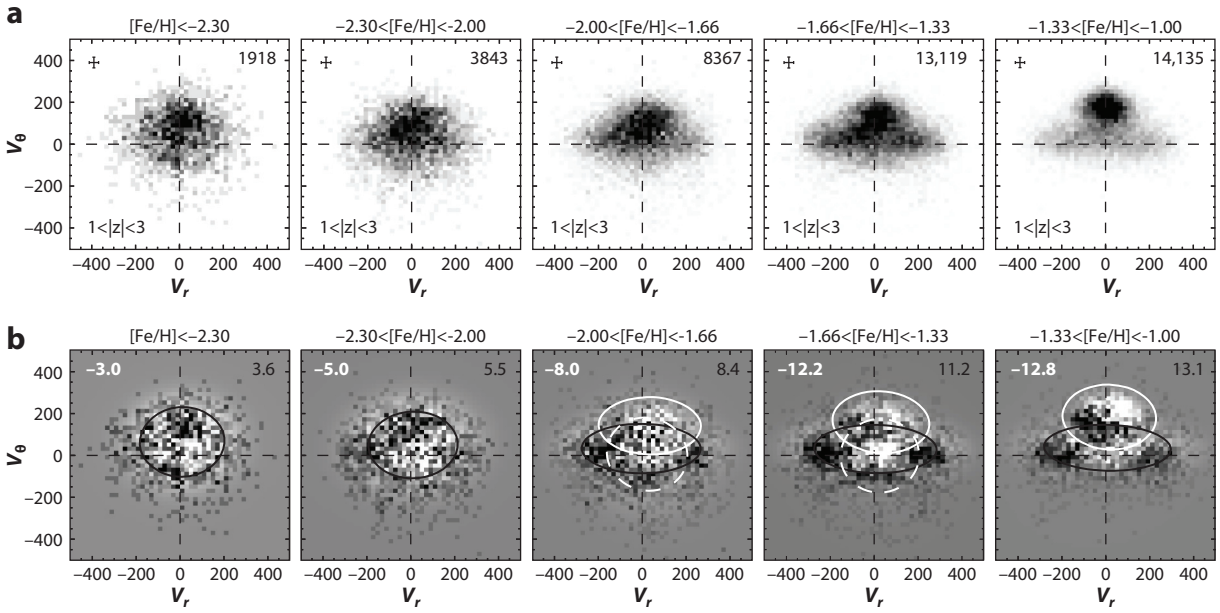

Figure 6

Map of the kinematics of halo stars in the sample used by Belokurov et al. (2018). This was obtained from the cross-match of the positions in *Gaia* DR1 and SDSS and use of the long time baseline to derive proper motions. Panel *a* shows the distribution for stars in different metallicity bins, while panel *b* shows the residuals resulting from a Gaussian mixture model, with the contribution of two and sometimes three subcomponents as indicated by the ellipses. Although a complex kinematic distribution can be retrieved statistically, comparison to **Figure 2*a*** using *Gaia* DR2 data reveals how the striking increase in quality of this data set leads to a true distinction of the various components, as was also noted in **Figure 5**. The V_R asymmetry seen in the rightmost panel of panel *b* for the faster moving component is also apparent in **Figure 2** and is likely the result of the impact of the Galactic bar on the kinematics of these stars, as reported by Antoja et al. (2015) for the canonical thick disk stars. Abbreviations: DR1, first data release; DR2, second data release; SDSS, Sloan Digital Sky Survey. Adapted from Belokurov et al. (2018), top panels of their figures 2 and 3.

et al. 2012, Hawkins et al. 2014, Vincenzo et al. 2019). The low-α stars were found to be younger than those in the thick disk. Since these are the most metal-rich stars and likely formed in Gaia-Enceladus before it was fully disrupted, this also dates the time of the merger and, at the same time, demonstrates that a disk was already in place in the Milky Way at this time, roughly 10 Gyr ago (see Gallart et al. 2019 and Section 5).

4.2.1.1. Dynamics of the merger. The details of the merger still have to be pinned down. For example, a coarse comparison of the *Gaia* kinematical data with existing simulations of the merger of a disk galaxy with a massive disky satellite (Villalobos & Helmi 2008, 2009), as shown in **Figure 8**, suggests that the merger was counter-rotating because the mean rotational motion of associated halo stars in the solar vicinity is (slightly) retrograde (see the sidebar titled Mean Rotational Velocity of Gaia-Enceladus Debris). The presence of specific features in velocity space, for example, the arc seen in **Figure 5*b***, and their resemblance to those seen in the simulations, support the retrograde infalling direction and also suggest that the merger's inclination was initially approximately 30°. However, other configurations might also be possible, as similar characteristics are found for a coplanar merger where the accreted object is spinning in the opposite sense than the host, as shown by Bignone et al. (2019) using the Evolution and Assembly of Galaxies and their Environments (EAGLE) cosmological simulations suite.

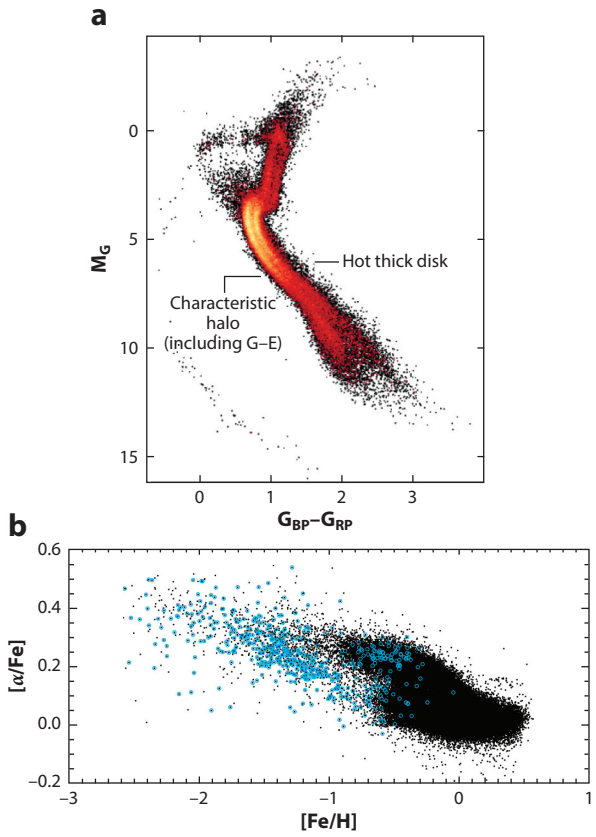

Figure 7

(*a*) The CMD from Gaia Collab. et al. (2018a), which revealed two sequences in a sample of stars kinematically selected to be part of the halo (with tangential velocities $V_T = 4.74\sqrt{\mu_{\alpha*}^2 + \mu_\delta^2}/\varpi > 200$ km s^{-1}). (*b*) When a selection in energy and angular momenta is performed (similar to that marked by the ellipse in **Figure 5*b***; for details, see Helmi et al. 2018 and their extended data figure 1), most of the stars in the blob region (*blue*) define a distinct sequence in [α/Fe] versus [Fe/H]. The stars in blue on the [α/Fe]-rich sequence correspond to thick disk stars on hot halo–like orbits, as discussed in Section 5. Panel *a* reproduced from Gaia Collab. et al. (2018a), reproduced with permission; © ESO; panel *b* adapted from Helmi et al. (2018). Abbreviations: CMD, color-magnitude diagram; G-E, Gaia-Enceladus.

Helmi et al. (2018) suggest a mass ratio of ∼4:1 for the merger (which has been confirmed by Gallart et al. 2019) on the basis of the estimated stellar mass of Gaia-Enceladus, the expected stellar mass–to-halo mass ratio for objects of this size, and the assumption that a $10^{10}\,M_\odot$ thick disk stellar mass is present at the time. Other authors have suggested stellar masses from $10^9\,M_\odot$ up to $5 \times 10^9\,M_\odot$ (Mackereth et al. 2019, Fattahi et al. 2019). Clearly these estimates are uncertain, but all point to a significant merger, with lower masses (as proposed by Donlon et al. 2019) being inconsistent with the chemical abundances of the stars (i.e., they would violate the mass-metallicity relation).[3] The exact configuration of the merger will have to be pinned down with

[3]This high metallicity and as the tightness of the α-poor sequence for [Fe/H] $\gtrsim -1.3$ (whose width is consistent with being due to measurement errors only) are the reasons why this debris is unlikely to have originated in several low-mass objects accreted on radial orbits.

GAIA-ENCELADUS/GAIA SAUSAGE

The prominence of Gaia-Enceladus was noticed by Belokurov et al. (2018) using an unpublished catalog of proper motions obtained by combining SDSS and *Gaia* DR1 astrometric positions (also used in Deason et al. 2017). Although the separation between the thick disk and the halo is less sharp because of the lower astrometric precision (as can be seen from **Figure 6**), the authors found (after performing a Gaussian mixture model), that a high fraction of the halo stars had very large radial motions. Through comparisons to zoom-in cosmological simulations, this significant radial anisotropy was interpreted as implying that the halo stars originated in a significant merger the Galaxy experienced between redshift 1 and 3. However, in the context of what was known before *Gaia* DR2, this was not the only possible interpretation, particularly because the lower quality of the proper motions did not reveal a mean retrograde (and hence somewhat abnormal) signal in the multi-Gaussian component decomposition, and chemical abundance information (in particular, the sequence of [α/Fe]) was not used in the study. As the authors themselves acknowledge in their paper, perhaps this blob or sausage structure, as it was called (see Myeong et al. 2018b, and the available versions on the arXiv), was the result of a monolithic-like collapse of the kind proposed by Eggen et al. (1962) (a scenario referred to hereafter as ELS) in the traditional model of the formation of an in-situ halo. The result of such a collapse would likely put the stars formed on radially biased orbits. Now, with the knowledge provided by *Gaia* DR2 data in combination with that of the APOGEE survey, which reveal, respectively, the retrograde mean motion of the halo and the distinct chemical sequence defined by the majority of its stars, there is absolutely no question that Belokurov et al. (2018) had seen Gaia-Enceladus's mark in the kinematics of halo stars and correctly interpreted its accreted origin with remarkable insight.

more detailed modeling and by probing the 3D motions and properties of stars well beyond the solar neighborhood.

In summary, the halo near the Sun (if not in a hot thick disk) is dominated by debris from Gaia-Enceladus, a very massive object that was accreted 10 Gyr ago. As such, it most likely represents the last significant merger that the Milky Way experienced. Probably after this was completed, the current Milky Way thin disk started a more quiescent growth phase, and this would be consistent with the ages of its oldest stars. Other large mergers the Milky Way has experienced since then include that with the Sagittarius dwarf, but because of the late the time of infall (~8 Gyr ago) and mass ratio of 1–5% ($M_\star \sim 5 \times 10^8\,M_\odot$; see, e.g., Dierickx & Loeb 2017, Fardal et al. 2019), this has resulted in a less dramatic impact. Even the ongoing merger with the Large Magellanic Cloud is less important (with a mass ratio is probably ~10%), although in both cases we do see their effect on the disk of our Galaxy, in the form of phase-space spirals[4] (Antoja et al. 2018) and waves (vertical and radial oscillations; see, e.g., Laporte et al. 2018a, Laporte et al. 2019; Bland-Hawthorn et al. 2019).

4.2.1.2. Evidence with hindsight. Besides Belokurov et al. (2018), several other authors had in fact come across traces of Gaia-Enceladus without knowing. We had a rather fragmented view of the inner halo until *Gaia* DR2 because it was based on small samples, and hence our knowledge was patchy and incomplete. For example, the sample with the low-α sequence of Nissen & Schuster (2010) contained fewer than 100 stars (which nonetheless was a significant increase in comparison to the original discovery paper, which had just 13 halo and 16 thick disk stars; see

[4]The authors originally called the structure discovered in *Gaia* DR2 near the Sun "snail-shell" (*caracol* in Spanish). This structure is a result of phase mixing, but because it is apparent in a slice of phase-space (the z-V_z plane), phase-space spiral might be preferred over phase spiral (see also Bland-Hawthorn et al. 2019, Khanna et al. 2019).

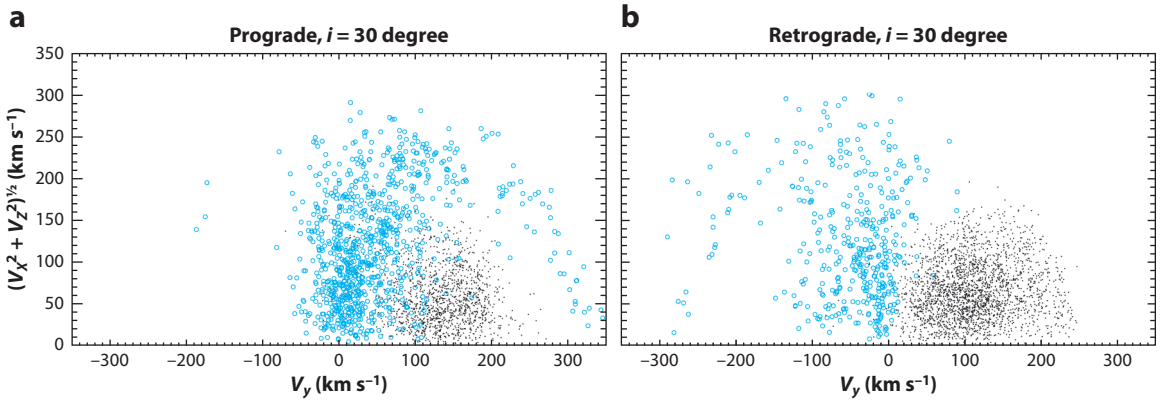

Figure 8

Toomre diagrams obtained from a set of simulations to study the formation of the Galactic thick disk via a 20% mass ratio merger (Villalobos & Helmi 2008). In these simulations, a merger between a disky satellite and a host disk is modeled for different orbital configurations. In panel *a*, the orbit is prograde, while in panel *b*, it is retrograde. In both cases the initial orbital inclination is 30°. The star particles plotted are located inside a solar neighborhood–like volume, 4 Gyr after infall, with black and blue corresponding, respectively, to those from the host and from the satellite. Some differences are apparent in the kinematic properties of the merger product, one of the most noticeable being the presence of an arc at high rotational velocities, positive for the prograde and negative for the retrograde case. This arc is composed of star particles lost early during the merger before the object had fully sunk in via dynamical friction (see Bos 2019). The arc in panel *b* is very reminiscent of that seen in the *Gaia* DR2 data shown **Figure 5*b***. Also, Bonaca et al. (2017, their figure 6) report the presence of a similar structure in the Latte cosmological simulation of a Milky Way–like galaxy, but its origin is not discussed in that paper.

Nissen & Schuster 1997). Although these authors were able to put forward a scenario rather similar to what has now been revealed with *Gaia* DR2 and APOGEE, it was not realized until recently that most of the halo follows the Nissen & Schuster low-α sequence, thanks to the work of Hayes et al. (2018) on the chemistry and Koppelman et al. (2018) on the kinematics (see also Haywood

MEAN ROTATIONAL VELOCITY OF GAIA-ENCELADUS DEBRIS

Determining the mean motion of the debris from Gaia-Enceladus is important as it reveals properties regarding the initial configuration of the merger. Support for a retrograde encounter is apparent from the comparison of the simulations shown in **Figure 8** with the data shown in **Figure 5*b***, as well as from the location of the vertical line (denoting null rotation) in the latter figure. To quantify this further, we select stars on the [α/Fe]-poor sequence, for [Fe/H] ≥ -1.3, i.e., the region dominated by Gaia-Enceladus debris (see **Figure 7**). By imposing a 20% relative parallax (or distance) error quality cut, using distances determined either via $1/\varpi$ or from the Bayesian method of McMillan (2018), a selection is made that satisfies $-500 \leq L_z \leq 500$ kpc km s^{-1}. The resulting sample is small but within 1 kpc of the Sun, $\langle v_\phi \rangle = -21.1 \pm 1.8$ km s^{-1} (6 stars) and within 2 kpc $\langle v_\phi \rangle = -16.1 \pm 2.8$ km s^{-1} (23 stars), where the uncertainty has been estimated from resampling the individual velocity errors. For the stars within 1 kpc, these errors are all smaller than 7.2 km s^{-1} (the mean is 3.3 km s^{-1}), while for those within 2 kpc, the mean error is 10.8 km s^{-1}. The signal is therefore weak but robust to measurement uncertainties (statistical and systematic) because within 1 kpc from the Sun, the parallax is $\gtrsim$1 mas, the relative errors are small ($\lesssim$20%) for the bright stars in the *Gaia* radial-velocity spectrometer (RVS) sample (Gaia Collab. et al. 2018d), and the systematic parallax bias (Lindegren et al. 2018, Arenou et al. 2018) is negligible within this parallax range (even if as large as 0.05 mas). A similar amplitude mean retrograde motion has been reported by Mackereth et al. (2019) using APOGEE distances.

et al. 2018). Possibly the reason for this is that the halo near the Sun is known to peak at a metallicity of [Fe/H] ~ -1.6 and have [α/Fe] $\sim 0.2 - 0.4$ around this iron abundance. Only at higher metallicity does the sequence by Gaia-Enceladus become clearly separate, with a lower [α/Fe] than the thick disk, as seen from in **Figure 7*b***. Other hints of this structure were present in the Chiba & Beers (2000) study based on Hipparcos data. The authors identified a concentration of stars for [Fe/H] ~ -1.7 with very high eccentricities ($e \sim 0.9$), but they interpreted it as being stars formed during an ELS-like collapse in the early Milky Way. Brook et al. (2003) compared the Beers et al. (2000) sample to a cosmological hydrodynamical simulation of the formation of a Milky Way–like galaxy. In this comparison, the authors identified a clump of stars with retrograde motions, which they proposed could be satellite debris. The presence of clumps of stars with retrograde motions goes back even further, to the work of, e.g., Majewski et al. (1996) and Carney et al. (1996) and more recently Kinman et al. (2007). The globular cluster Omega Centauri became the natural culprit because it was known to have a retrograde orbit and because of its peculiar multiple populations, which led to the suggestion that it could have been the nucleus of a disrupted dwarf galaxy (Dinescu 2002, Bekki & Freeman 2003, Meza et al. 2005).

4.2.2. The dual halo. The two sequences revealed in the CMD (Gaia Collab. et al. 2018a) are a direct reminder of the suggestion of a dual halo in the Milky Way. As just discussed, it has been possible to attribute the first, more metal-poor sequence largely to Gaia-Enceladus. However, the second sequence is populated by stars that, kinematically, are clearly part of the tail of the thick disk seen in **Figure 5*b***(Di Matteo et al. 2019, Haywood et al. 2018).

The idea of a dual halo was discussed quite thoroughly by Norris (1994) (see also the nice historical introduction in Carollo et al. 2010). Norris (1994), like several other authors around the same time, found that at lower metallicities, the retrograde component becomes more and more prominent. In his interpretation of the data, this dual halo would consist of an accreted component (as in Searle & Zinn 1978) and a contracted halo (as in the ELS model of Eggen et al. 1962).

We now know from the *Gaia* DR2 data that what Norris (1994) called the contracted halo is actually largely heated (proto–)thick disk. So it was indeed formed mostly in situ; however, the stars did not form during a collapse but in a disk that was heavily dynamically perturbed during a merger, as in the simulations of Zolotov et al. (2009) and Tissera et al. (2013). In contrast, the accreted component is predominantly debris from Gaia-Enceladus. This explains why the local inner halo was long considered to be slightly prograde (since it is a mix of prograde thick disk and slightly retrograde Gaia-Enceladus, and was concealed as a single component because of large velocity errors, as shown in **Figure 5*a***) and more metal-rich locally than in the outskirts. In comparison, the debris from Gaia-Enceladus dominates farther out (at several kpc away from the Sun and above the Galactic plane), implying that the outer halo consists of more metal-poor stars on retrograde orbits (at least in comparison to the proto–thick disk). This is also what Morrison et al. (2009) found in a carefully constructed sample of nearby metal-poor RGB stars with accurate distances, and what the more recent study by Bonaca et al. (2017) using *Gaia* DR1 data (Gaia Collab. et al. 2016) revealed.

Carollo et al. (2007, 2010) and Beers et al. (2012, and references therein) put the idea of a "dual halo" on firmer ground based on SDSS and SEGUE data, despite concerns that the retrograde mean motion signal was driven by biases in the distances, as suggested by Schönrich et al. (2011). The *Gaia* DR2 data put the debate fully to rest since the retrograde signal is very strong and is also seen in the nearby halo, where the distances have been measured very precisely and accurately with trigonometric parallaxes (or with Bayesian methods; McMillan 2018). There is, however, still some tension with the work of Carollo et al. (2007) because what they called the outer halo peaked at a metallicity of [Fe/H] ~ -2.2, lower than is typical for Gaia-Enceladus stars. A possible

way out would be to consider that large galaxies like Gaia-Enceladus probably had a metallicity gradient. As the galaxy was destroyed, some of the material in the outer regions would be put on more unbound orbits. This material would have lower metallicity and form part of the outer portions of the inner halo (here we refer to the inner halo as that within 20 kpc of the Sun). Other possibilities could be an issue with the metallicity scale calibration, or perhaps a small bias in the sample selection, which, because it is based mostly on the colors for main sequence turn-off stars, might preferentially select more metal-poor stars (Lee et al. 2019).

4.2.3. More substructures in the inner halo. Several smaller substructures have been identified in the nearby halo. They are discussed in this section.

4.2.3.1. Helmi streams. The first genuine accreted inner halo kinematic substructures discovered near the Sun were the Helmi streams[5] (Helmi et al. 1999). Before their discovery, there had been reports of substructure (e.g., Majewski et al. 1994), and in particular, Eggen argued for the presence of streams in the halo, but their reality was often questioned because of the methods used (because in some cases, for example, the very uncertain distances were enforced to match those expected for a kinematic group[6]). The Helmi streams were identified in a data set largely compiled by Chiba & Yoshii (1998), who used the Hipparcos data set supplemented by line-of-sight velocities and distances from the literature. The streams are also readily apparent in *Gaia* DR2 (Gaia Collab. et al. 2018c, Koppelman et al. 2018). A characteristic of the streams is that they have rather high z-velocities, which makes them easy to identify as they are well separated from the rest of the stars with the same rotational velocity ($v_\phi \sim 150$ km s^{-1}). One of the streams has positive v_z while the second (and better populated) has $v_z < 0$. Koppelman et al. (2019b) showed that the streams likely stem from a progenitor of $M_* \sim 10^8$ M$_\odot$. Seven globular clusters have been associated with this object, including NGC 5024 and NGC 5053 (Koppelman et al. 2019b, Massari et al. 2019). These clusters follow a well-defined age-metallicity relation, and their number is consistent with that expected from the globular clusters' specific frequency relation given the progenitor's mass (see, e.g., Zaritsky et al. 2016). The time of infall estimated by Koppelman et al. (2019b) is between 5 and 8 Gyr ago (see also Kepley et al. 2007) and it is largely driven by the asymmetry seen in the number of stars with positive and negative v_z. It is somewhat puzzling that an object that is not so massive would have made it to the inner halo so recently. Since its orbit seems to lie close to a resonance (Hagen 2020), the inferred timescale could be underestimated as streams will then have spread out more slowly. Alternatively, the progenitor system may have fallen in together with a heavier galaxy as part of a group (as is the case for the Magellanic Clouds; Sales et al. 2017).

Enough members of the Helmi streams are now known that it is possible to produce a well-populated CMD, which is very similar to those constructed for many decades for the dwarf spheroidal satellites of the Milky Way (Tolstoy et al. 2009) as shown in **Figure 9*a***. The information contained in this CMD should allow us to derive a star formation history. In combination with the metallicity distribution function shown in **Figure 9*b***, this should enable the reconstruction of the full chemical history of the system (in a similar manner as done for several dwarf spheroidal galaxies in, e.g., Homma et al. 2015). Detailed elemental chemical abundances (such as those measured by Roederer et al. 2010), might also help in this respect (see, e.g., Lanfranchi

[5]This name has been used informally in workshops and conferences for years, and it appears in print in Klement (2010).

[6]It would nonetheless be an interesting exercise to revisit, in a systematic fashion, the Eggen moving groups with the data newly available, particularly from *Gaia* DR2. For example, Navarrete et al. (2015) analyzed the Kapteyn group and the chemical abundances of its stars and showed that they do not really constitute a physical unity.

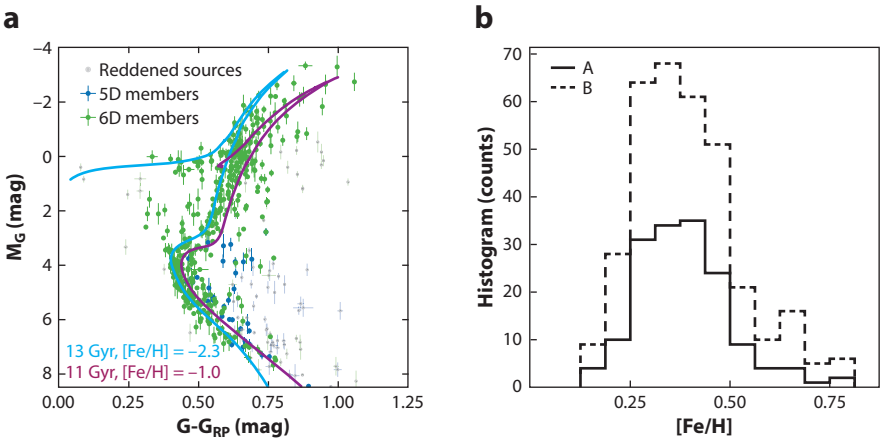

Figure 9

Properties of the stars from the Helmi streams. (*a*) CMD of members identified in a sample with 6D coordinates (from *Gaia* DR2 and supplemented further by radial velocities from RAVE, APOGEE and LAMOST), in green. Members identified using the 5D sample from *Gaia* DR2 in fields within 15° of the (anti)center are plotted in blue. Highly reddened members are indicated in light gray. The isochrones serve to illustrate that the Helmi streams include a range of old, metal-poor stellar populations. (*b*) This is confirmed by showing the metallicity distribution function using the APOGEE/RAVE/LAMOST data sets. The two distributions marked A/B correspond to two different selections in IoM space. Both peak at [Fe/H] ∼ −1.5 and reveal a broad range of metallicities. Adapted from Koppelman et al. (2019b), with permission; © ESO. Abbreviations: APOGEE, Apache Point Observatory Galactic Evolution Experiment; CMD, color-magnitude diagram; IoM, integrals of motion; LAMOST, Large Sky Area Multi-Object Fibre Spectroscopic Telescope; RAVE, Radial Velocity Experiment.

& Matteucci 2010). It is intriguing that such an exercise of reconstructing the star formation and chemical enrichment history is now possible using nearby stars for long-gone objects. This truly lies at the heart of what it means to carry out Galactic archaeology.

4.2.3.2. Other reports of kinematic substructures. Several other kinematic substructures have been reported in the literature prior to *Gaia* DR2. Typically, though, these structures were less conspicuous as they were based on Hipparcos/Tycho data in combination with ground-based radial velocities (see the reviews by Klement 2010, Smith 2016). Kepley et al. (2007) and Morrison et al. (2009) report lumpiness in a sample of RGB stars with accurate distances, some of which can be attributed to Gaia-Enceladus and to the hot thick disk, but some of which are outliers on very prograde orbits. Re Fiorentin et al. (2015) report substructures among the fastest-moving halo subdwarfs. More recently other authors used LAMOST and TGAS (the Tycho-Gaia astrometric solution) (Liang et al. 2017), RAVE and TGAS (Helmi et al. 2017), and SDSS and *Gaia* DR1 (Myeong et al. 2018a) and identified several small clumps, some of which were related to those previously known (e.g., the S2 group in Myeong et al. 2018a, which overlaps very substantially with the Helmi streams). Other small kinematic groups in *Gaia* DR2 have also been identified by Koppelman et al. (2018), Borsato et al. (2020), and Yuan et al. (2020).

4.2.3.3. Sequoia and Thamnos. Two of the clumps identified by Koppelman et al. (2018) may be part of a larger substructure associated with the debris of a dwarf galaxy dubbed Sequoia (Myeong et al. 2019). The associated stars have more retrograde motion and a lower metallicity than Gaia-Enceladus, as can be seen in **Figure 10**, and they are on a less eccentric orbit. Myeong

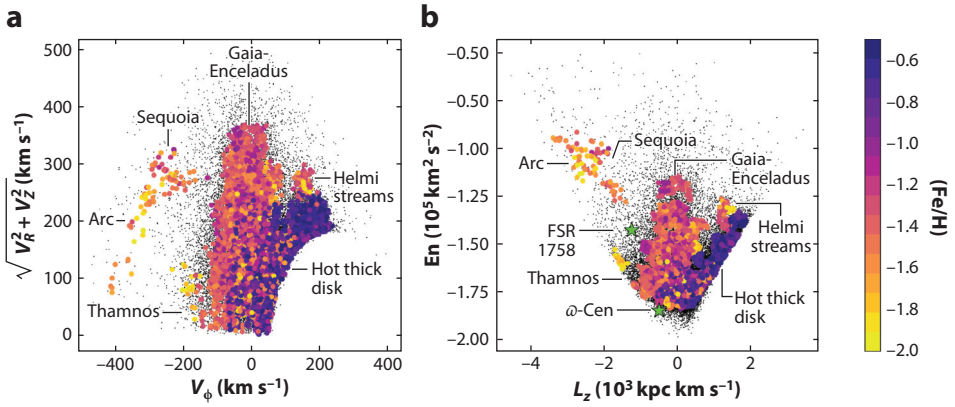

Figure 10

Distribution of halo stars selected kinematically, i.e., $|\mathbf{V} - \mathbf{V}_{\rm LSR}| > 180$ km s^{-1}, within 3 kpc, and with $\varpi/\sigma_\varpi > 5$, from the *Gaia* RVS sample extended with radial velocities from APOGEE, RAVE, and LAMOST, with metallicities from the latter. Panel *a* shows their distribution in the Toomre diagram, while panel *b* shows energy E and z angular momentum. Stars identified by HDBSCAN to be in clumps in the space of E, L_z, eccentricity, and [Fe/H] are color-coded by [Fe/H], with the rest shown as black dots (for details, see Koppelman et al. 2019a). The arrows indicate the approximate locations of the various groups discussed in the text. Comparison of their extent in E-L_z to N-body simulations suggest that $M_\star \sim 6 \times 10^5$ M$_\odot$ for Thamnos and $M_\star \sim 10^7$ M$_\odot$ for Sequoia. Adapted with permission from Koppelman et al. (2019a), with permission; © ESO. Abbreviations: APOGEE, Apache Point Observatory Galactic Evolution Experiment; LAMOST, Large Sky Area Multi-Object Fibre Spectroscopic Telescope; LSR, local standard of rest; RVS, radial-velocity spectrometer.

et al. (2019) suggest that Omega Centauri could have been Sequoia's nuclear star cluster and that several other clusters, including the recently characterized large cluster FSR 1758 (Cantat-Gaudin et al. 2018, Barbá et al. 2019), would also be associated. However, Massari et al. (2019) argue that it is more likely that Omega Centauri is associated with Gaia-Enceladus, given its location in the age-metallicity diagram of the Galactic globular clusters. As can be seen in **Figure 10*b***, the extent of Sequoia in the space of energy and L_z, if the two clusters were associated with it, would be as large as that of Gaia-Enceladus, implying that it would need to have been as massive (for details, see Koppelman et al. 2019a). This, however, would be in tension with its lower metallicity.

The presence of additional debris (besides Gaia-Enceladus) with retrograde motions (Myeong et al. 2019) to a certain extent confirms the analysis by Mackereth et al. (2019) of a data set that is the cross-match of APOGEE DR14 and *Gaia* DR2. Taking advantage of the chemical abundance information provided by APOGEE, these authors have applied a *k*-means algorithm to identify clustering using [Fe/H], [Mg/Fe], [Al/Fe], and [Ni/Fe] as well as eccentricity. Mackereth et al. (2019) found evidence for the presence of a group of stars with low eccentricity and high [Mg/Fe], of which roughly 50% have (very) retrograde motions (with the rest likely associated with the thick disk).

Meanwhile, Matsuno et al. (2019), using chemical abundances from the SAGA database (Stellar Abundances for Galactic Archeology; **http://sagadatabase.jp/**) (see Suda et al. 2008 and subsequent papers), showed that the high-energy, more retrograde stars have lower [Mg/Fe] at [Fe/H] $\lesssim -1.6$ than Gaia-Enceladus stars and, especially, different [Na/Fe]. The authors further argue that the other elemental abundances are too different from those measured for Omega Centauri for the cluster (which has a higher binding energy) to be related.

THE VERY RETROGRADE HALO

A possible scenario to explain the findings reported in this section is the existence of (a bonsai) Sequoia, as embodied by a clump of high-energy retrograde stars that is truly distinct from Gaia-Enceladus (because of the differing [Na/Fe] abundances reported by Matsuno et al. 2019), but whose extent is smaller than that originally proposed by Myeong et al. (2019). It is not inconceivable that the region of the arc-like structure contains a mix of debris from two different objects, stars from the outskirts of Gaia-Enceladus and from the Sequoia galaxy. An alternative possibility is that we are seeing only stars from the outskirts of Gaia-Enceladus and that these followed a somewhat different chemical enrichment path. The lower-energy region, with stars of low eccentricity and high [Mg/Fe] identified by Mackereth et al. (2019) and Koppelman et al. (2019a), would then be associated with Thamnos.

Finally, Koppelman et al. (2019a) report evidence that the lower-energy region occupied by stars tentatively associated with Sequoia is likely part of a different separate structure, which the authors call Thamnos (see **Figure 10**). Thamnos stars define the separate clump to the lower left of the region occupied by Gaia-Enceladus ($v_y \sim -150\,\mathrm{km\,s^{-1}}$ and $v_\perp < 150\,\mathrm{km\,s^{-1}}$). Their progenitor was likely a small galaxy accreted on a low-inclination orbit, and this is consistent with the lower mean metallicity of its stars. Thamnos, which in ancient Greek means "shrubs," also overlaps in part with substructures reported by Helmi et al. (2017) and Koppelman et al. (2018). The majority of the low-eccentricity stars with high [Mg/Fe], low metallicity, and retrograde motions identified by Mackereth et al. (2019) overlap with those from Thamnos.

Figure 10 also reveals that some of the stars from Sequoia overlap directly with the arc-like structure assigned to Gaia-Enceladus on the basis of the resemblance to numerical simulations, as discussed before. If Gaia-Enceladus had a metallicity gradient, which might be expected given that it was of comparable size to the Large Magellanic Cloud, then one might expect the outskirts to be more metal poor and part of the material lost first to be on a more a retrograde orbit, as found for some Sequoia stars (see the sidebar titled The Very Retrograde Halo).

The above discussion demonstrates the field's high state of flux and that it is currently in some turmoil. It shows that it is very difficult, given the available data and methods, to pin down the origin of the different clumps and overdensities being discovered in the halo near the Sun. This is particularly manifested in the analysis of Yuan et al. (2020), who identified more than 50 small clumps using neural network–based clustering on the very metal-poor sample of stars from LAMOST. Nonetheless, it is possible that very detailed modeling and chemical analysis of a large sample of stars will help shed light on their true nature. At the moment, the modeling is sketchy, carried out in idealized (time-independent or non-cosmological) configurations; often hydrodynamics and star formation (as well as chemical enrichment) are not followed, and the numerical resolution (especially in terms of particle number) is typically too low to do a proper comparison with the features seen in the data. Furthermore, the samples with detailed and precise chemical abundances of halo stars, even for those that are bright and nearby, are relatively small. Finally, more robust statistical or probabilistic tools are needed to assign stars to overdensities, as these very likely have some degree of overlap in phase-space.

4.2.4. Substructures in the outer halo. At larger distances from the Sun, i.e., in the outer halo, many overdensities have been uncovered, especially with photometric wide-field surveys such as SDSS. Examples are the Sagittarius streams (Ivezić et al. 2000, Yanny et al. 2000), Hercules Aquila Cloud (Belokurov et al. 2007) and the Virgo overdensity (Vivas et al. 2004, Jurić et al. 2008). At this point, the nature of these high-latitude structures (beyond the Sagittarius streams) and

the link to those in the solar vicinity discussed in previous sections remains unknown, although Simion et al. (2019) have proposed that both Hercules-Aquila and Virgo are related to Gaia-Enceladus. To pin this down will require large samples of stars with accurate, full phase-space information, some of which will become available in future *Gaia* data releases combined with data from large spectroscopic surveys such as WEAVE (William Herschel Telescope Enhanced Area Velocity Explorer; **https://ingconfluence.ing.iac.es:8444/confluence//display/WEAV/The+WEAVE+Project**) (Dalton et al. 2016), 4MOST (4-metre Multi-Object Spectroscopic Telescope; **https://www.4most.eu/**) (de Jong et al. 2019), DESI (Dark Energy Spectroscopic Instrument; **https://www.desi.lbl.gov/the-desi-survey/**) (Levi et al. 2019), and smaller efforts like the H^3 survey of Conroy et al. (2020). Again, orbital integrations and extensive modeling are needed to understand what is what.

Other known overdensities located closer to the Galactic plane are the Monoceros ring (Newberg et al. 2002) and the feathers at slightly higher latitudes (seen in SDSS and in Pan-STARRS, respectively; Grillmair 2011, Bernard et al. 2016). These low-latitude structures are likely the result of the response of the disk to a massive perturber, such as Sagittarius, and perhaps also contain some satellite debris (Sheffield et al. 2018, Laporte et al. 2018b).

Besides large overdensities, many thin streams crisscrossing the halo at larger distances have been uncovered (see Grillmair & Carlin 2016, Shipp et al. 2018). These include, for example, GD-1, Atlas, Orphan, Pal 5, and many more. Mateu et al. (2018) also identified 14 candidate streams using RR Lyrae stars and produced a very interesting and useful interface, the `galstreams` footprint library and toolkit for Python (**https://github.com/cmateu/galstreams**) to visualize and keep track of all known structures. An example of the distribution on the sky of currently known streams and spatial substructures is shown in **Figure 11**. Thin streams tell us the story of the destruction of less massive objects, i.e., smaller dwarf galaxies and globular clusters, and are particularly useful for constraining the Galactic potential and the distribution of mass at large radii. An exciting development is the detection of substructure, gaps, and overdensities in these streams, potentially revealing the presence of (dark) satellites orbiting the halo of the Milky Way (Bonaca et al. 2019).

The `STREAMFINDER` algorithm developed by Malhan & Ibata (2018) has also allowed the discovery of less distant thin streams. These include Gaia-1 and Gaia-2 (Malhan et al. 2018) and the stream from Omega Centauri itself (Ibata et al. 2019). `STREAMFINDER` works by randomly sampling radial velocities (which have not been measured for the majority of the stars in *Gaia* DR2) while making use of the proper motion and photometric information of stars (i.e., for a given color, there are at most 3 possible absolute magnitudes; for details, see Ibata et al. 2019). From these tentative phase-space coordinates, orbits are integrated in a Galactic potential, and if stars can be found along the orbit on a spaghetti- or stream-like structure, then a stream is identified (after proper statistical assessment and comparison to a suitable background).

4.2.5. Link between inner and outer halo (sub)structures. Several authors, including Watkins et al. (2009) and Deason et al. (2013), have reported the presence of a break in the density profile of the Galactic stellar halo at a distance of ∼20–25 kpc from the Galactic center. Deason et al. (2018) demonstrated that likely marks the orbital turning points (i.e., a shell) of the debris from Gaia-Enceladus. The authors integrated the orbits of the stars belonging to the Sausage (Gaia-Enceladus) and showed that their apocenters lie at roughly this distance. Several shells might be expected from the debris, possibly at different distances because the object must have experienced significant dynamical friction. This break also manifests itself in a change in the shape of the velocity ellipsoid of halo stars around this distance, as reported by Kafle et al. (2014).

0: **VOD/VSS**	1: **Monoceros**	2: **EBS**	3: **Her–Aq**	4: **PAndAS**	5: **Tri–And**	6: **Tri–And2**	7: **PiscesOv**	8: **EriPhe**
9: Phoenix	10: WG1	11: WG2	12: WG3	13: WG4	14: Acheron	15: Cocytos	16: Lethe	17: Styx
18: ACS	19: Pal15	20: Eridanus	21: TucanaIII	22: Indus	23: Jhelum	24: Ravi	25: Chenab	26: Elqui
27: Aliqa Uma	28: Turbio	29: Willka Yaku	30: Turranburra	31: Wambelong	32: Palca	33: Jet	34: Gaia-1	35: Gaia-2
36: Gaia-3	37: Gaia-4	38: Gaia-5	39: PS1-A	40: PS1-B	41: PS1-C	42: PS1-D	43: PS1-E	44: ATLAS
45: Ophiucus	46: Sangarius	47: Scamander	48: Corvus	50: Sgr-L10	51: Orphan	52: Pal5	53: GD-1	54: Tri/Pis
55: NGC5466	56: Alpheus	57: Hermus	58: Hyllus	59: Cetus	60: Kwando	61: Molonglo	62: Murrumbidgee	63: Orinoco
64: Phlegethon	65: Slidr	66: Sylgr	67: Ylgr	68: Fimbulthul	69: Svol	70: Fjorm	71: Gjoll	72: Leiptr

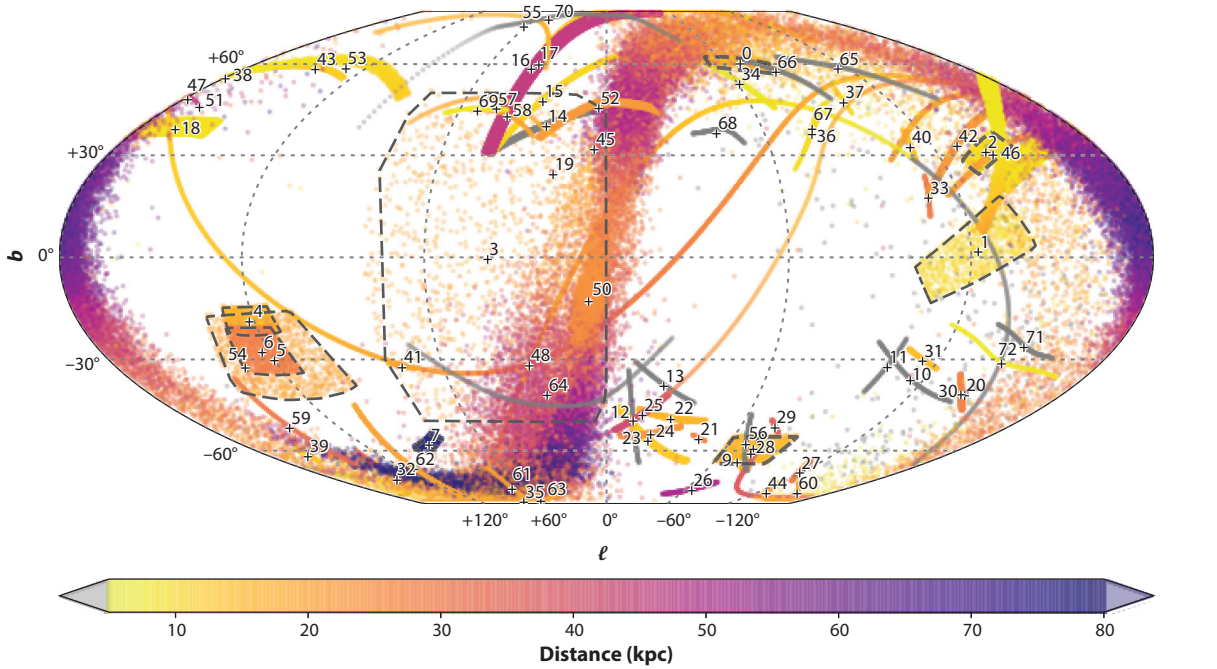

Figure 11

Sky distribution of currently known spatially coherent streams and overdensities (indicated as regions delimited by dashed lines, and in boldface in the inset) produced using the `galstreams` package by Mateu et al. (2018). Adapted with permission from C. Mateu and E. Balbinot.

In an attempt to make the link between the outer and the inner stellar halo even stronger, we have followed a similar approach to that of Deason et al. (2018) and have integrated the orbits of halo stars located within 1 kpc of the Sun. Since we expect the inner halo to be well mixed, these stars' trajectories should give us a broader view of the 3D (spatial) structure of the halo, for example. This is much in the same way that orbits can be seen as the building blocks of a galaxy in Schwarzschild's modeling (Schwarzschild 1979) and can be used to reproduce, for example, their light profile.

The top panel of **Figure 12** shows the orbits of all stars from *Gaia* DR2 located within 1 kpc from the Sun with halo-like kinematics, defined as having $|\mathbf{V} - \mathbf{V}_{\rm LSR}| > 210$ km s^{-1}. In this case, we have used the distances from McMillan (2018). We have used their current positions and velocities (corrected for the Solar motion and the LSR) as initial conditions for the orbital integrations. These were performed in the Milky Way Gala potential (Price-Whelan 2017, Price-Whelan et al. 2019), which contains a Navarro–Frenk–White halo, a nucleus, and a disk and bulge (Bovy 2015). The integration covers 2 Gyr. We have plotted each orbit sampled in 0.1-Gyr intervals, color-coded by their distance from the Sun. The top panel of **Figure 12** reveals

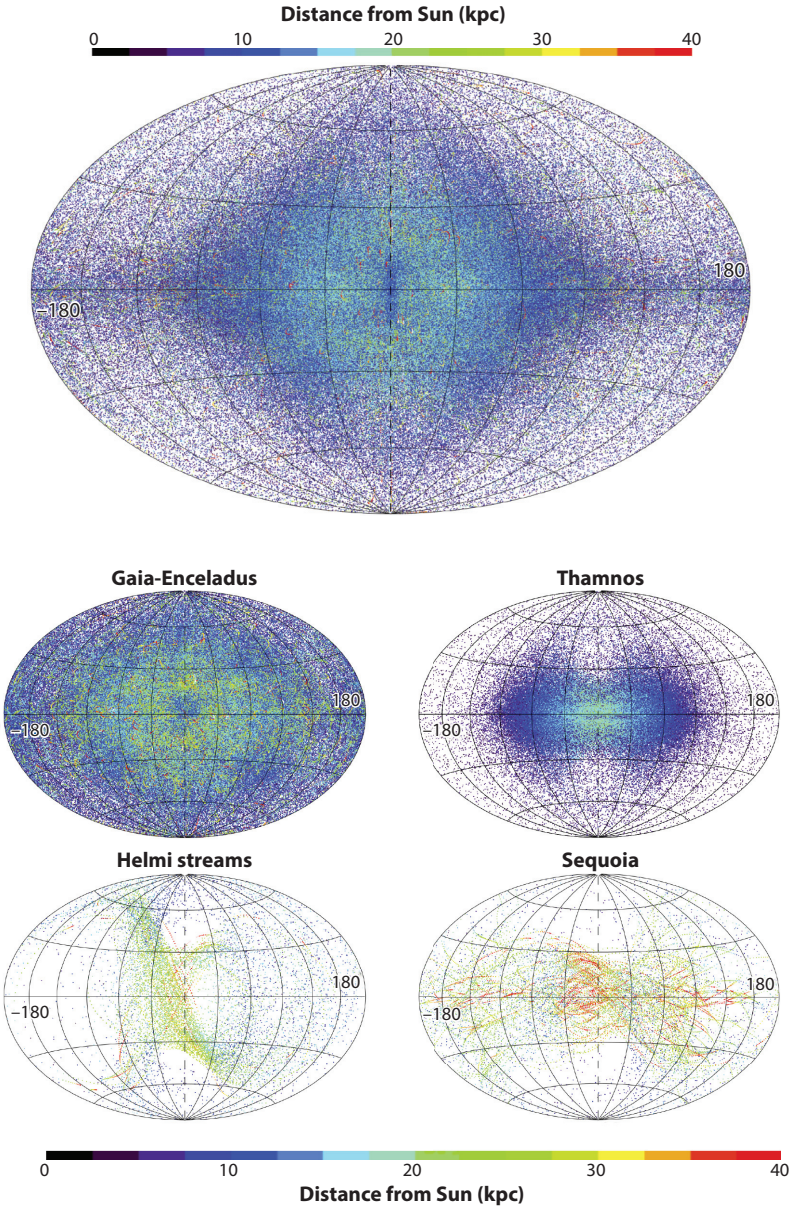

Figure 12

Sky projections in Galactic coordinates (l, b) of the orbits of stars with halo-like kinematics currently located within 1 kpc of the Sun (and with $|L_z| \geq 10$ kpc km s^{-1}). The orbits have been integrated in a Milky Way–like potential for 2 Gyr, and each point in the diagram corresponds to a point on a star's orbit color-coded by its distance. In the top panel, we show all the stars together, while in the four lower panels, we have separated the stars in the structures identified thus far following the assignment of Koppelman et al. (2019a), which is similar to that schematically shown in **Figure 10**. The decrease in the density of points toward the Galactic center is not physical and is due to removal of stars ($\lesssim$1.3%) with very radial orbits of low $|L_z|$ angular momenta.

the presence of many overdensities, boxy shapes, and some sharp edges, some of which bear some resemblance to those seen in the distribution of RR Lyrae in Pan-STARRS by Sesar et al. (2017) and shown in **Figure 13*a***.

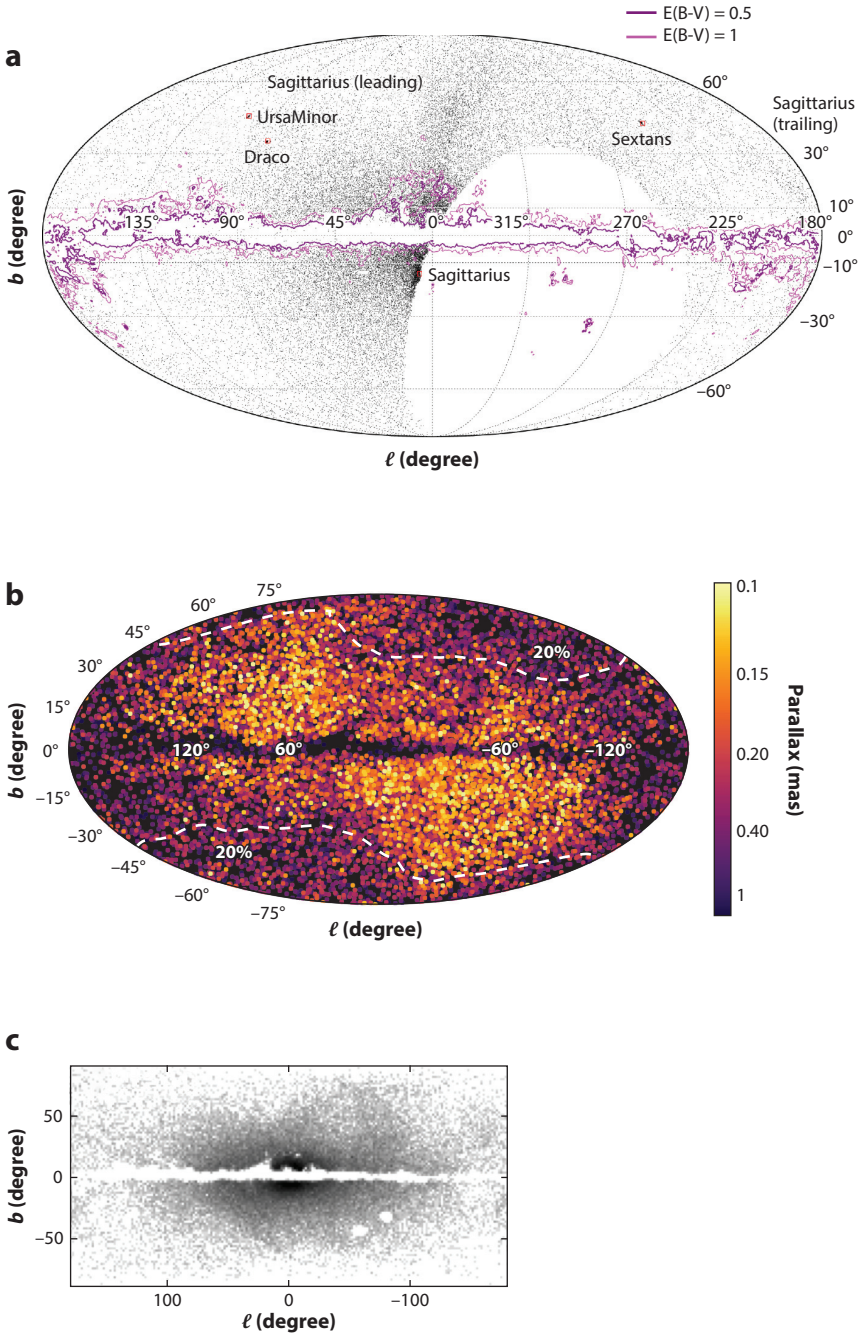

(*Caption appears on following page*)

Figure 13 (*Figure appears on preceding page*)

(*a*) Distribution of RR Lyrae stars from Pan-STARRS. Adapted with permission from Sesar et al. (2017) and from the AAS. (*b*) Distribution of potential members of Gaia-Enceladus from *Gaia* DR2 (with $-1{,}500 < L_z < 150$ km s^{-1} kpc) and with parallaxes >0.1 mas. The color coding indicates parallax, with more distant stars in yellow. The white contour encompasses 90% of all stars in the 6D *Gaia* DR2 sample with $0.1 < \varpi < 0.2$ mas and 20% relative parallax error. Tentative members of Gaia-Enceladus follow a similar distribution on the sky as all the distant stars, implying that the parallax quality cut introduces a selection bias: Distant stars outside of these contours could be missed because these regions of the sky have been visited less frequently by *Gaia*. Figure adapted by H.H. Koppelman and this author from Helmi et al. (2018), their figures 3 and 4. (*c*) Distribution of RR Lyrae from *Gaia* DR2, after removal of the Sagittarius streams and other satellites of the Milky Way. A similar selection effect is apparent in this figure. Adapted with permission from Iorio & Belokurov (2019), top right panel of their figure 1.

The bottom four panels of **Figure 12** show the orbits of stars now separated by the progenitor they are presumably associated with according to Koppelman et al. (2019a) (i.e., roughly following what is shown in **Figure 10**). Comparison of the panels reveals that these four objects do indeed have different orbital properties as they have deposited their debris in different spatial configurations. For example, the debris from Gaia-Enceladus follows a symmetric configuration with respect to Galactic latitude $b = 0^o$, with sharp boundaries at Galactic longitude $l \sim \pm 120^o$. The limited extent in longitude is similar to that reported by Helmi et al. (2018) and shown in **Figure 13*b***. This map shows the sky distribution of stars selected to be part of Gaia-Enceladus (with relative parallax errors <20%, and with a rather generous cut on L_z toward the retrograde halo and a sharper, more conservative one toward prograde moving stars to avoid contamination from the hot thick disk). The remarkable difference with the sky map obtained via the orbit integration is the degree of incompleteness and the effect of selection biases, particularly for distant stars (with $\varpi \lesssim 0.2$ mas) that appear as a result of the imposed parallax quality cut. Incompleteness also affects the RR Lyrae map of Iorio & Belokurov (2019) shown in **Figure 13*c***, although in this case it is due to poorer time sampling and hence characterization of their light curves in *Gaia* DR2. This explains the significant asymmetries with respect to the Galactic plane seen **Figure 13*b*** and *c*, which are not consistent with the estimated time of accretion and the size of the progenitor, as its debris is expected to have fully phase mixed. This is indeed what the velocities of nearby stars from Gaia-Enceladus predict, as shown in **Figure 12** (as pointed out by H.-W. Rix, private communication). Meanwhile, the distributions in longitude revealed in the studies of Helmi et al. (2018), Iorio & Belokurov (2019), and Sesar et al. (2017) are not too dissimilar to that predicted for Gaia-Enceladus, as seen in **Figure 12**. They all reveal a very centrally concentrated distribution of the debris.

Figure 12 could also serve as guidance in searches for associated debris, particularly at large radii. Furthermore, since the exact location of the features is sensitive to the gravitational potential, a comparison between the outcome of the orbit integrations and observational data (position in the sky, distance, and kinematics of the various features) could be used to constrain better the distribution of mass in the Milky Way. Some of the features may even link to the overdensities discussed in the literature and already mapped at larger distances from the Sun, as a coarse comparison with **Figure 11** suggests.

5. THE THICK/EARLY DISK

Not many review articles have been written on the Galactic thick disk (but a good starting point is the introduction of Robin et al. 2014). This is likely because its reality (independent of that of

the thin disk) has been highly debated over the years (Gilmore & Reid 1983, Bahcall & Soneira 1984) and also recently (Fuhrmann 2011, Bovy et al. 2012). Another likely reason is that conflicting answers regarding its properties have sometimes been obtained depending on the type of observational tool used to characterize its properties (abundances, kinematics, star counts; see, e.g., de Jong et al. 2010, Cheng et al. 2012). This is discussed by Kawata & Chiappini (2016), and an insightful explanation is given by Minchev et al. (2015). We do not attempt to provide a review here and instead focus on observational facts and recent discoveries, particularly in relation to the stellar halo, which help us understand, at least in part, the formation and evolutionary history of this component.

5.1. Overview of Its Properties

The thick disk was discovered through star counts by Gilmore & Reid (1983). These authors found an excess of stars at large heights above the plane, beyond what would be expected from a single exponential fit corresponding to the thin disk. The excess could be fit by invoking a second component that also had an exponential functional form, but with a larger scale height. Subsequent work revealed that the stars in the thick disk had different kinematics that, although mostly rotationally supported, have lower rotational speeds (by about 30–50 km s^{-1}) and higher velocity dispersions than the thin disk. The first spectroscopic studies showed that the thick disk is more metal poor than the thin disk and is composed of older stars [see, e.g., section 4 of the extensive review by Gilmore et al. (1989)].

More detailed high-resolution chemical elemental abundance studies demonstrated that thick disk stars organize themselves in a segregated sequence from that of the thin disk stars in the solar neighborhood in, for example, [α/Fe] versus [Fe/H] (Gilmore et al. 1995). Several authors have recently provided definitive evidence that the sequences are truly separate, and hence that the two components really are physically distinct, as they are made up of stars that do not overlap in their properties (e.g., Adibekyan et al. 2011, Recio-Blanco et al. 2014, Hayden et al. 2015). Haywood et al. (2013) also showed that the stars in the thin and thick disks follow very tight and well defined tracks in [α/Fe] and [Fe/H] with age, with a break occurring at ∼8–9 Gyr, which marks the oldest stars present in the thin disk. These distributions display a small scatter, a result that, although based on a local sample, can be extended beyond the solar vicinity since the orbits of the stars probe a relatively large radial range (from 2–10 kpc from the Galactic center). This small scatter (which implies no radial gradient) can be explained if the majority of thick disk stars formed rather quickly in a massive gaseous disk, possibly supported by turbulence (Snaith et al. 2014).

The thick disk metallicity near the Sun peaks at [Fe/H] ~ -0.5 and extends on the metal-rich side up to solar metallicity. It also has a very significant tail, which is often referred to as the metal-weak thick disk (Norris et al. 1985, Morrison et al. 1990, Morrison 1993, Beers et al. 2002). The stars associated with this tail are clearly visible as the data points with high [Mg/Fe], [Fe/H] $\lesssim -1$, and low eccentricity in **Figure 14**, which is based on APOGEE data (Mackereth et al. 2019). This metal-weak thick disk could potentially be related to the very first disk or the oldest disk that was ever formed in the proto–Milky Way.

5.2. Formation Paths

Typically, four different scenarios are discussed in the literature for the formation of the thick disk (Gilmore et al. 1989, Robin et al. 2014). The traditional and oldest is that it formed via a minor merger onto a preexisting disk, which leads to dynamical heating and the formation of a hotter but still rotation-supported component (Quinn et al. 1993). The accretion scenario is based on

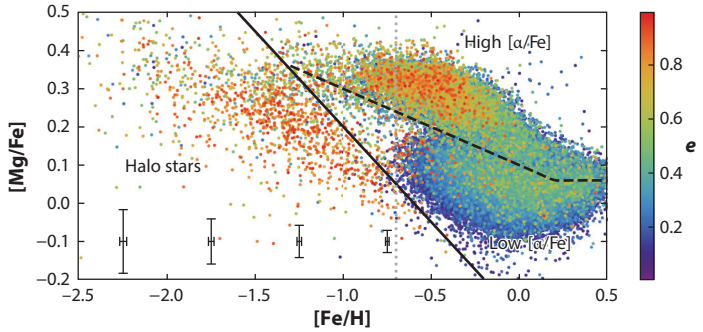

Figure 14

Distribution of [Mg/Fe] versus [Fe/H] color-coded by eccentricity using APOGEE and *Gaia* data. Notice the presence of low-eccentricity stars (*blue/green*) for [Fe/H] $\lesssim -1$, many of which appear to be following a well-defined sequence that appears to be the extension of the traditional thick disk toward lower metallicity. Note as well the increase in scatter in [Mg/Fe] for [Fe/H] $\lesssim -1.75$. The vertical line indicates the highest metallicity considered for the sample used to perform a *k*-means analysis that reveals the presence of high- and low-eccentricity populations among halo stars, as discussed in Section 4.2.3.3 Adapted with permission from Mackereth et al. (2019), their figure 1. Abbreviation: APOGEE, Apache Point Observatory Galactic Evolution Experiment.

cosmological simulations, which showed that if satellites are preferentially accreted from specific directions, this can lead to their debris being deposited in a planar configuration (Abadi et al. 2003). On this preferred plane, gas would later cool down and form the thin disk. The gas-rich scenario is inspired by cosmological hydrodynamical simulations that show that disks were highly turbulent and hotter in the past, partly because they were more gas rich and partly because of the ongoing merger activity that prevented full settling (Brook et al. 2004, Bird et al. 2013). This is also what observations of high-redshift disks appear to suggest (e.g., Bournaud et al. 2007). A final scenario is that of migration, that is stars from the inner (thin) disk have migrated with time to the outer regions of the disk. Because of inside-out formation and metallicity gradients, these stars would be older and have different chemical composition. Schönrich & Binney (2009) were the first advocates of this model who have quantitatively explored its feasibility.

Sales et al. (2009) proposed that the dominant formation mechanism of the thick disk could be determined from the eccentricity distribution of its stars. They showed that the different paths discussed above lead to different distributions, with radial migration only slightly changing the low eccentricities of the stars. In contrast, a dry large minor merger would leave behind a distribution of stars with intermediate eccentricity (the heated disk) and a high-eccentricity bump formed mostly by accreted stars. A comparison with data from RAVE and SDSS carried out later by Wilson et al. (2011) and Dierickx et al. (2010) showed that the most likely path was through gas-rich mergers, i.e., turbulent disks in which stars were forming during mergers (Brook et al. 2004). This interpretation and idea have been largely confirmed by the latest analyses based on *Gaia* DR2. As Gallart et al. (2019) showed, the majority of the thick disk stars likely formed during/after the merger with Gaia-Enceladus and not before. However, some fraction did form before, as in the dry merger scenario, although the predicted bump at high eccentricity associated with the accreted stars (Sales et al. 2009, Di Matteo et al. 2011) is not seen in the thick disk. In fact, these stars exist, but now we know they make up a large fraction of the Galactic halo (i.e., this is Gaia-Enceladus debris). It is interesting that the connection between the thick disk and halo had not been fully

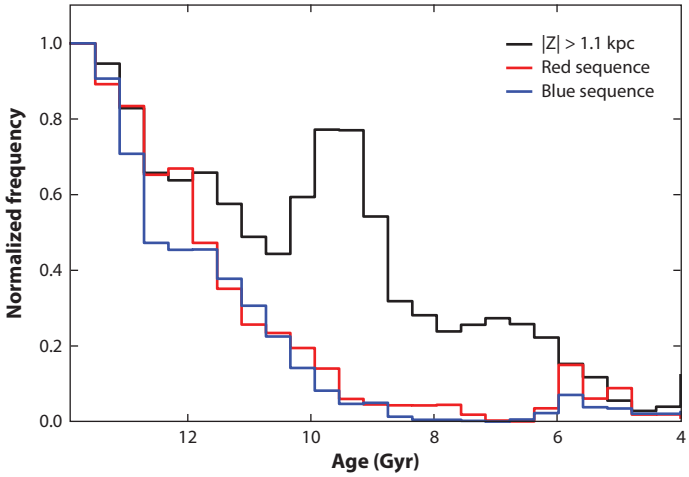

Figure 15

Age distribution for stars with $|Z| > 1$ kpc and $V_T < 200$ km s^{-1} (i.e. the thick disk, *black*) and for stars on the red and blue halo sequences (with $b > 30^o$ and $V_T > 200$ km s^{-1}) as derived from the analysis of *Gaia* DR2 photometric data. The stars on the blue and red sequences, which correspond to Gaia-Enceladus and to the hot thick disk respectively, are both old but have different colors because of their different metallicities. The thick disk proper (*black*) is younger and more metal rich. This figure reveals agreement with earlier work showing that the youngest stars in Gaia-Enceladus are 9–10 Gyr old (the tail for younger ages is likely contamination), and also shows that a starburst in the thick disk appears to have been triggered 10 Gyr ago. This was probably the time of the closest encounter between the two interacting systems, after which Gaia-Enceladus was fully engulfed by the Milky Way. Figure adapted by T. Ruiz Lara and C. Gallart from Gallart et al. (2019), left panel of their figure 2.

made until recently (although see Purcell et al. 2010, who using numerical simulations discussed this possibility).

Although it is probable that radial migration has played some role in the evolution of the thick disk, and that some fraction of the stars in the thick disk have an (inner) thin disk origin (see e.g., Adibekyan et al. 2011), it is likely that the efficiency of this process was initially overestimated (as argued by Minchev et al. 2012). The evidence discussed above, particularly the work of Gallart et al. (2019), supports a scenario in which a gas-rich disk experienced a merger with Gaia-Enceladus, where the stars already present were dynamically heated, and star formation was triggered (possibly in a starburst), leading to the formation of the bulk of the stars in the thick disk. This interpretation is based on what is shown in **Figure 15**. This figure shows that the distribution of stellar ages in the thick disk proper peaks at ∼10 Gyr, while the stars in the hot thick disk (the red sequence shown in **Figure 7*a*** and reported by Gaia Collab. et al. 2018a), have similar, older ages to those in Gaia-Enceladus (i.e., the blue sequence, shown in **Figure 7*b***).

This scenario is also consistent with the rather uniform distribution of [α/Fe] with age and radius discussed by Haywood et al. (2015), as such a merger likely triggered a global response of the whole disk. Although there was probably a large amount of radial migration during the merger as the disk became dynamically hotter, this migration (only blurring, no churning) would not have been due to internal mechanisms, as proposed by Schönrich & Binney (2009), but externally induced.

5.3. Further Insights on the Early Disk from Chemistry and Dynamics

The evidence accumulated so far and discussed above suggests that we may have identified the existence of the proto-disk as the metal-weak (or hot) thick disk, and that this was present more than 10 Gyr ago. It is interesting that relatively low-eccentricity stars have survived as such the dynamical impact of a massive minor merger,[7] allowing this disk to be traced back to lower and lower metallicities, as **Figure 14** shows. In fact, in recent work on ultra-metal-poor stars (with [Fe/H]<-4), Sestito et al. (2019) showed that a fair fraction (26%) actually are rotationally supported and have thick disk-like kinematics. These stars potentially trace the most pristine disk in the Milky Way. It will be interesting to bridge the gap in metallicity between the metal-weak thick disk and the regime probed by the most metal-poor stars to trace the history of the very first disk-like component in our Milky Way. This is particularly relevant in the context of linking the Milky Way to studies of high-redshift disks (e.g., van Dokkum et al. 2013, Lehnert et al. 2014, Pillepich et al. 2019).

Just like we have done for the halo, we can now put previous work on the thick disk in the recently gained context. For example, Gilmore et al. (2002) discovered an excess of stars toward the rotation fields (i.e., $l \sim 90^o, 270^o$), with lags of approximately 100 km s^{-1} (as well as a minor contribution from a retrograde component). They argued this is due to shear in the kinematics of the thick disk such that at higher latitudes ($b \sim 33^o, 45^o$), thick disk stars rotate more slowly than near the plane. They interpreted this as evidence for a shredded satellite, but instead (given the evidence we have discussed so far), it is likely they were seeing kicked-out thick disk stars and a bit of debris from Gaia-Enceladus. They were nonetheless "deciphering the last major invasion of the Milky Way," as the title of their paper suggested. Further analysis of Wyse et al. (2006) and Kordopatis et al. (2013) toward other lines of sight confirmed their first results. Other evidence hinting at the dynamical consequences of a significant merger on the early disk is provided by the overdensities discovered by Larsen & Humphreys (1996) and Larsen et al. (2011) suggesting that the thick disk may be triaxial. Such a configuration is not an uncommon end product of simulations of disks experiencing a massive minor merger (Villalobos & Helmi 2008). In these simulations, this shape is delineated only by some of the stars already present at the time of the merger, which, as Gallart et al. (2019) argue, do not comprise the majority of the thick disk of the Milky Way.

Other evidence of substructure in the thick disk was put forward by Schuster et al. (2006), who identified two different groups of stars in the thick disk with different mean metallicities and mean rotational velocities. This is one of the key papers preceding the Nissen & Schuster (2010) discovery of the two sequences, since what Schuster et al. (2006) were seeing was, in fact, stars from Gaia-Enceladus and from the thick disk. Analysis of the Geneva-Copenhagen survey (Nordström et al. 2004) led Helmi et al. (2006) to also propose the presence of substructure in the region kinematically dominated by thick disk stars. In a follow up paper (Helmi et al. 2014), these authors demonstrate that there is a transition in the dynamical properties of stars at a metallicity of [Fe/H] ~ -0.4. Below this value, stars have a large range of eccentricities, while above it, stars are only on low-eccentricity orbits. There is also significantly more scatter in [α/Fe] below this [Fe/H] value, as if there were a mix of populations (as shown by Mackereth et al. 2019, reproduced here in **Figure 14**). Bearing in mind differences in metallicity scales, this is the [Fe/H] at which a clear distinction can be made between stars formed before and after

[7] However, this is not fully unexpected, as the simulations of Villalobos & Helmi (2008) show that a thin disk–like component remains 15–25% intact after the merger is completed.

the merger with Gaia-Enceladus (Gallart et al. 2019). Only the thick disk stars below this value (i.e., more metal poor) have been kicked out on to more extreme orbits (and there may even be some contamination from Gaia-Enceladus; see Di Matteo et al. 2019). Meanwhile, stars formed at higher metallicities formed and have stayed on proper thick disk–like orbits. This was not the original interpretation given by Helmi et al. (2014) (and follow-up papers such as Stonkutė et al. 2012, 2013 and Ženovienė et al. 2015), who attributed the features to the presence of merger debris, whereas we now believe the latter is a minor contributor; what is seen is simply the imprint of an important transition in the history of the disk (in fact, similar conclusions using different orbital parameters were reached earlier by Liu & van de Ven 2012).

This is an important point as there has been some propensity to attribute substructure or overdensities to accretion events. As vehemently argued by Jean-Baptiste et al. (2017), this is not necessarily the case. A merger can also induce asymmetries and substructure in the populations formed in situ (as shown by, e.g., Gómez & Helmi 2010, Gómez et al. 2012, and for the thick disk, simulations of Villalobos & Helmi 2008). Asymmetries and substructures can also arise from internal dynamical processes such as resonances with, for example, the Galactic bar, which is responsible for the Hercules stream (Dehnen 2000). Stars in the thick disk are also affected by the bar, as shown by Antoja et al. (2015) and as evidenced in **Figure 2*a***, where the v_R velocity distribution of the (hot) thick disk is clearly asymmetric in the same way as the thin disk, whose asymmetry is explained as being due to the bar.

The above discussion serves to stress that care is required in the interpretation of substructure. Nonetheless, if substructures can be proven to be related to mergers, this would be interesting from the archaeological point of view. As just discussed, such substructures can reveal the response of both the in situ system (and hence contain information about its properties and the nature of the encounter) and the accreted population.

6. DISCUSSION

Gaia DR2 data, supplemented with data from existing large spectroscopic surveys, have made it relatively straightforward to identify what was plausibly a very important milestone in Galactic history: the merger with Gaia-Enceladus. Stars from Gaia-Enceladus distinguish themselves kinematically with slightly retrograde and very eccentric orbital motions, and more patently via their chemical abundances. In particular, these stars define a tight chemical sequence in [α/Fe] versus [Fe/H], which is especially apparent for [Fe/H] $\gtrsim -1.3$. The sequence merges with that of the (metal-weak) thick disk for lower metallicities, and the values of [α/Fe] here depict significantly more scatter (see **Figure 14**). It seems improbable that the scatter is due to the overlap of stars from just these two systems (as each follows a tighter relation at higher metallicities); more likely, it is indicative of other accretion events, whose debris may have been identified already in part (as discussed in Section 4.2.3). Because of the correlations between mass and metallicity and between mass and star formation history, small-mass objects will have lower average values of [Fe/H] (hence populate the [Fe/H] $\lesssim -1.3$ regime), and also typically show lower [α/Fe] due to their less-efficient star formation. Both these facts seem to be consistent with the findings reported above.

Nissen & Schuster (1997) were among the first to show that α-poor stars are interesting markers for accretion events, and as discussed by Ishigaki (2019), large surveys are helping to identify larger numbers of low-α stars, which are then being followed up with high-resolution spectroscopic observations (see, e.g., Xing et al. 2019). Similarly, r-process enhanced stars are receiving more attention (see, e.g., Sakari et al. 2018), particularly because the large scatter present in the

field halo population at very low metallicities may indicate several accreted small galaxies (see, e.g., Roederer et al. 2018). Carbon-enhanced metal-poor (CEMP) stars also provide interesting insights, although their formation channels are not yet fully understood. For example, most CEMP-no stars (CEMP stars with no overabundance of neutron capture elements) have [Fe/H] $\lesssim -2.5$, while the CEMP-s stars (enhanced in s-process elements) typically have [Fe/H] > -2.5(Aoki et al. 2007). Since s-process elements would be produced on longer timescales, such stars would have their origin (when not in a binary) in systems that have sustained star formation longer, i.e., more massive hosts, and thus would be preferentially found in the inner halo (supported by the recent analysis of Lee et al. 2019). In contrast, CEMP-no stars form more predominantly in low-mass galaxies (hence their lower average metallicity) which, when accreted, would remain in the outer regions of the halo because they would not be able to sink in via dynamical friction (see e.g., Starkenburg et al. 2017), which appears to be in line with the trends observed in the Milky Way halo (Carollo et al. 2014).

The general picture emerging of a few large building blocks dominating the inner stellar halo, with Gaia-Enceladus as possibly the largest, is consistent with that expected from cosmological simulations for a galaxy like the Milky Way. Zoom-in cosmological hydrodynamical simulations such as Auriga (Grand et al. 2017) and FIRE (Feedback in Realistic Environments) (Hopkins et al. 2014), or those based on *N*-body methods combined with semianalytic models such as Aquarius (Cooper et al. 2010), are very useful for understanding the general properties of stellar halos and how they might relate to, for example, merger history (Tissera et al. 2013, Pillepich et al. 2015, El-Badry et al. 2018). Some of these simulations are beginning to find Milky-Way look-alikes in terms of their merger history, as reported, for example, by Fattahi et al. (2019). Large, fully cosmological hydrodynamical simulations, such as the Illustris suite and its successor IllustrisTNG (Naiman et al. 2018, Nelson et al. 2019) also contain Milky Way–like galaxies. The largest EAGLE cosmological simulation (Schaye et al. 2015), for example, contains 100 objects that are close analogs to the Milky Way in terms of stellar and dark mass, SFR, and bulge-to-disk ratio, of which a handful have dynamically similar stellar halos (see Bignone et al. 2019).

The evolution of the galaxy identified by Bignone et al. (2019) in the EAGLE suite as a good Milky Way look-alike is shown in **Figure 16** around the time it merges with a Gaia-Enceladus analog. The panels of the figure show the evolution of the SFR and stellar mass (**Figure 16*a*** and ***b***, respectively) for the different components identified according to the circularity of their stellar orbits. At the time of the merger, there is a significant increase in the SFR in the whole system, with that of the fiducial thin disk increasing dramatically toward the end of the merger (fueled in part by gas from the accreted object, which also helps its further growth). Both panels show that all components are affected by the merger, suggesting the existence of populations in the thick disk and bulge that are coeval with the timing of the merger.

The figure also shows that the Gaia-Enceladus analog barely completes two orbits before it is fully disrupted. Its mass ratio in this simulation is only 20%, and both the host and the infalling object have more than 50% of the baryons in cold gas. Such an event is thus quite different from those typically modeled in the context of dwarf galaxy accretion for various reasons. First, the debris is expected to be much more complex. On the one hand, because of dynamical friction, stars lost early might have different eccentricities (and lower metallicities), and hence their orbits differ from those lost later on. On the other hand, intricate tidal tail morphologies become apparent when a disky galaxy is accreted (Quinn 1984). Second, the gas responds strongly, and it is conceivable that some star formation might take place in the tidal arms or that the formation of star clusters may be triggered. The degree of complexity of such an event evidences the need for tailored simulations including gas, star formation, and chemical evolution to fully interpret and model the observations currently available.

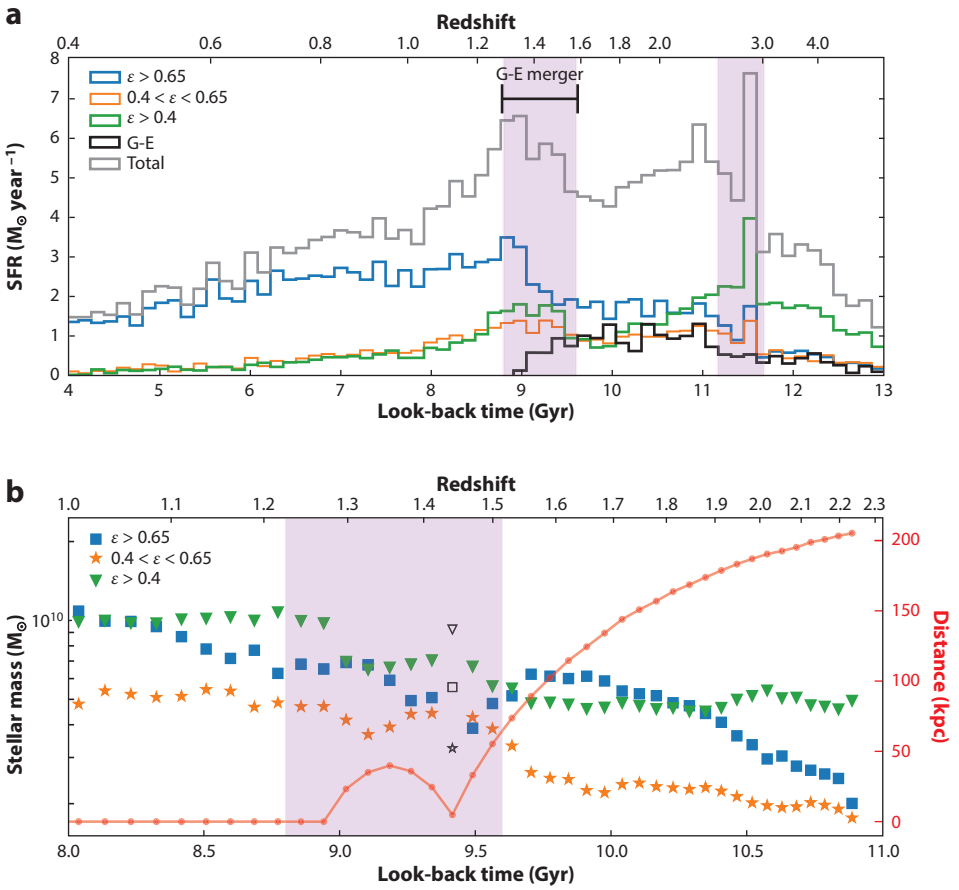

Figure 16

Evolution of a Milky Way–like galaxy identified in the largest EAGLE cosmological simulation. The galaxy's spheroid component has dynamical properties similar to those of the Milky Way (a significant population of stars on very eccentric orbits, i.e., the Gaia Sausage) as the result of a merger with another system that was completed at $z \sim 1.2$. Stars have been associated with components on the basis of the circularity of their orbits (computed at each point in time), with low circularity (*green*) corresponding to the spheroid, intermediate (*orange*) representing the thick disk, and high (*blue*) the thin disk. The thick disk in this simulation originates in part from a heated disk (star particles transferred from the thin disk and put on less circular orbits during the merger), but also from stars formed during the merger itself. Panels *a* and *b* show the increase in the SFR and stellar mass, respectively, of all components, particularly during the merger. Adapted with permission from Bignone et al. (2019) and reproduced with permission from the AAS. Abbreviations: EAGLE, Evolution and Assembly of Galaxies and their Environments; G-E, Gaia-Enceladus; SFR, star formation rate.

6.1. Next Steps: Simulations

Because of their limited resolution, many of the cosmological simulations just mentioned have been resampled to produce more particles (Lowing et al. 2015, Grand et al. 2018, Sanderson et al. 2020) as a star particle in a recent simulation is typically seen as representing a stellar population of approximately 10^3–10^4 $M_\odot$. Nonetheless, important limitations remain, including the ability to trace the true phase-space distribution of stars originating in objects with a stellar mass lower than 10^6 $M_\odot$ or thereabouts. Furthermore, not all these simulations follow chemical enrichment

properly, and as discussed in previous sections, this is necessary to guide the interpretation of newly-identified structures now and in the future.

The study by Bignone et al. (2019) makes clear that cosmological simulations (even with low resolution) are also useful for exploring or making links between the formation paths of the different Galactic components. Now that the identification of true analogs in cosmological simulations has become possible, it will be of great interest to carry out new zoom-in simulations of these objects. They will allow us to address a variety of questions, including gas physics, star formation, and chemical enrichment processes, as well as to establish the true links between different events in the assembly history of the Milky Way. Furthermore, such simulations will be necessary to guide dark matter detection experiments, which often assume that the dark matter particles follow Maxwellian velocity distributions. We now know that the stellar halo near the Sun is complex and has multiple kinematic components (see, e.g., O'Hare et al. 2020 for a discussion of the impact on direct detection experiments). The halo has stars with kinematics corresponding to the tail of the thick disk and to a component that is mildly retrograde, which is associated to Gaia-Enceladus. But we do not know how the dark matter should be distributed given the particular Galactic history just unraveled (although see Necib et al. 2019a). It is therefore very important to carry out such simulations now that the amount of freedom has been significantly reduced and the boundary conditions are better known so that we can provide concrete constraints on the initial conditions. Such simulations can also be used to understand some of the Milky Way's peculiarities, such as the possibly fairly low mass of the supermassive black hole in the center of the Galaxy, the distribution of satellites, and the origin of their configuration.

6.2. Next Steps: Statistical Analyses

To trace the assembly history of the Milky Way as far back as possible, it will also be necessary to work in a more systematic fashion than the current one. This is essential for establishing, for example, the mass spectrum of the objects accreted and their internal characteristics. It will require the application and development of statistical methods, some of which are available in the literature (e.g., IoM, frequency space); Fourier analysis; machine learning; and clustering algorithms such as HDBSCAN (Hierarchical Density-Based Spatial Clustering of Applications with Noise) (as used by Borsato et al. 2020, Koppelman et al. 2019a, Necib et al. 2019b) or those based on neural networks (Yuan et al. 2020). An important aspect is the assessment of the statistical significance of a given feature or clump, and this can be done through comparison with either models or suitably randomized samples. It would also be useful if there were more consistency in the different structures reported in the literature. Sometimes a structure is reported as newly discovered but has been reported before (for a recent example, see O'Hare et al. 2020). This leads to confusion in the field (in the naming and the reality of the features) and also does not help in building up a coherent picture of Galactic history. A possible improvement would be to assign membership probabilities to the different stars and to publish these together with the different structures and stars' IDs.

Similar issues arise for the globular cluster population of the Milky Way. Although Massari et al. (2019) tentatively associated many (at least 35%) of the globular clusters of the Milky Way with what we may identify as the main building blocks of the halo (at least near the Sun)—Gaia-Enceladus, Sagittarius, the Helmi Streams, and Sequoia—for many globular clusters, the assignment is not unique, particularly in IoM space (see, e.g., Myeong et al. 2018b). More precise ages for the clusters could potentially be useful because although the age-metallicity relations are well defined, they are not fully unambiguous (see Kruijssen et al. 2019).

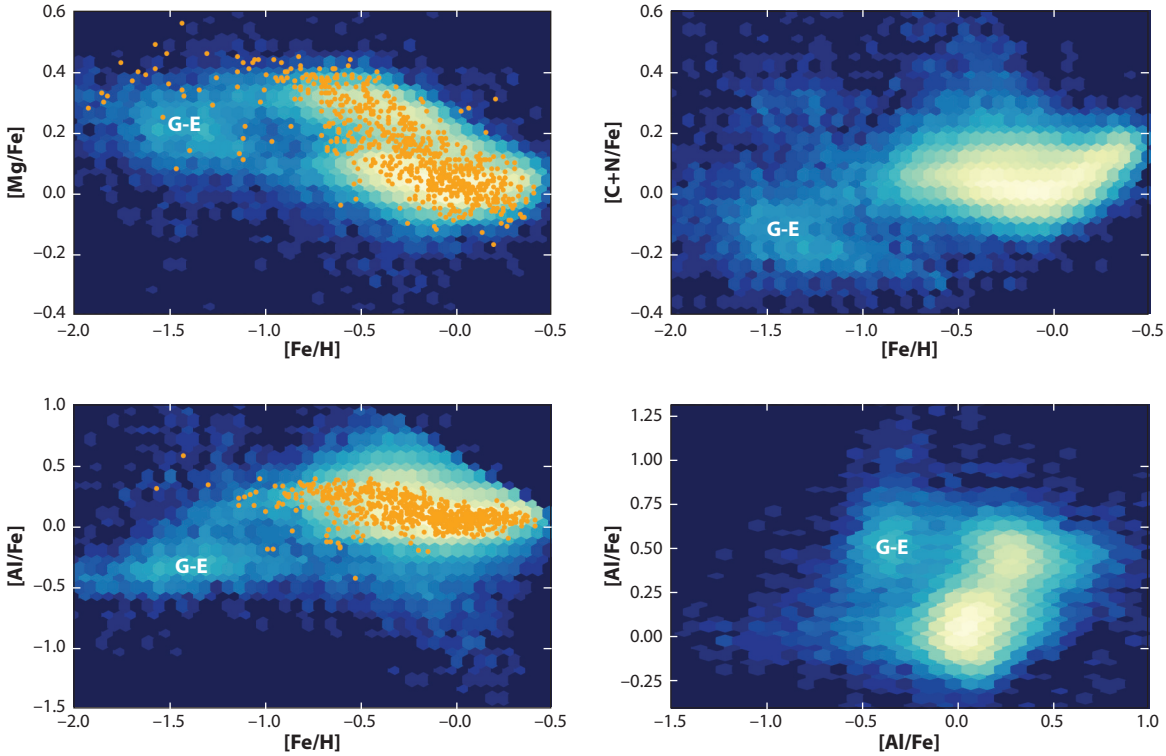

Figure 17

Two-dimensional abundance distribution of APOGEE DR14 stars in different chemical abundance planes. The filled orange circles correspond to kinematically selected disk stars from Bensby et al. (2014). Note the presence of G-E and its clear distinction from the thick disk, not only in [Mg/Fe] versus [Fe/H] but also in lighter elements such as [Al/Fe] and [C+N/Fe]. Adapted with permission from Das et al. (2020), their figure 3. Abbreviations: APOGEE, Apache Point Observatory Galactic Evolution Experiment; DR, data release; G-E, Gaia-Enceladus.

For the interpretation of the various structures, it is clear that there is an urgent need for detailed chemical abundances of the stars with full phase-space information. Such samples will also aid in disentangling the different merger events, assessing their origins (particularly if substructures overlap in, e.g., IoM space, as will necessarily happen in the majority of cases), and characterizing their properties and history. A very nice example of what is currently possible along these lines was given by Das et al. (2020). Their analysis of APOGEE DR14 data is shown in **Figure 17**, where the different main structures discussed in this review are clearly separated in chemical abundance space.

6.3. Next Steps: Surveys

The need for spectroscopic surveys of large numbers of stars has been recognized since the pioneering ideas of Freeman & Bland-Hawthorn (2002) and discussed in the context of, for example, ESO-ESA (European Southern Observatory-European Space Agency) synergies by Turon et al. (2008). This interest has led to a significant increase in the number and scope of surveys. Surveys such as RAVE, SEGUE (Sloan Extension for Galactic Understanding and Exploration), and Gaia-ESO (**https://www.gaia-eso.eu**) have been carried out over the past decade; some, like

APOGEE, LAMOST, and GALAH have been running over the past several years. In the next few years, projects such as WEAVE, 4MOST, and DESI using 4-m class telescopes and MOONS (Multi Object Optical and Near-infrared Spectrograph; **https://vltmoons.org**) on the VLT (Very Large Telescope) will see the light. The Galactic surveys that will be carried out using these facilities have two complementary goals. The first is to obtain the missing radial velocities for stars for which *Gaia* has (at best) measured the 5D phase-space location. The second goal is to obtain high-resolution spectra for brighter stars to do chemical labeling and characterization of the most metal-poor populations, for example, in the halo. The first goal is important for the dynamics of distant halo stars, for which tangential velocity constraints available from *Gaia* data releases will be available but less precise. The radial velocity measurements will allow mapping of the mass distribution in our Galaxy at large radii (Helmi et al. 2019). Also, for nearby faint dwarf stars, obtaining the missing radial velocity component is useful because such stars could be used to trace the time variations in the gravitational potential of the Milky Way in frequency space, as discussed in Section 3.3.

Furthermore, high-resolution spectroscopic follow-up is of utmost importance, as the discovery of Gaia-Enceladus has taught us. It is arguably the most powerful way to fully pin down the history and to identify debris with certainty, as well as to disentangle accretion events from one another. The high-resolution surveys planned by, e.g., WEAVE and 4MOST will be carried out using relatively bright stars, i.e., down to $G \sim 16$, because of the use of 4-m class telescopes (see, e.g., Christlieb et al. 2019). Although these surveys will be invaluable, it is already clear that a wide-field spectroscopic survey on an 8–12-m class telescope would be fantastic as it would really match the capabilities of *Gaia* and, e.g., LSST (the Large Synoptic Survey Telescope; **https://www.lsst.org**) (Ivezić et al. 2019) in the coming years. In particular, for the identification and characterization of debris from low-mass systems, it will be necessary to target main sequence stars, as they are much more numerous than the few RGB stars present in ultrafaint-like galaxies. Such galaxies are particularly interesting because of questions related to the presence of thresholds for galaxy evolution and the impact of reionization and feedback processes, and because they may host some of the most metal-poor stars. These stars reveal the imprint of just a few SNe and possibly of the initial mass function in the early Universe. Because of the low densities of tidal debris and of the stellar halo more generally, follow-up must be carried out using a wide field, and an 8–10-m telescope may well necessary to reach the required depth. The PFS (Prime Focus Spectrograph; **https://pfs.ipmu.jp/intro.html**) on Subaru (Tamura et al. 2016) is an instrument that could potentially help with the chemical labeling, although its highest-resolution mode has resolution $R \sim 5{,}000$ and so obtaining detailed chemical abundances for many elements will not be feasible. The MSE (Maunakea Spectroscopic Explorer; **https://mse.cfht.hawaii.edu**; see **https://mse.cfht.hawaii.edu/misc-uploads/MSE_Project_Book_20181017.pdf**) is another interesting facility being considered, but there are no other concrete plans at the time of writing of this review, although Pasquini et al. (2018) discuss in some detail a concept developed at ESO whose main science driver is high-resolution follow-up of *Gaia* targets, in a case termed "the Milky Way as a model galaxy organism."

7. CONCLUSIONS

Enormous progress has been made in recent years in our understanding of the evolution of the Milky Way from the perspective of the stellar halo and thick disk. This has been possible particularly thanks to *Gaia* DR2 and the many spectroscopic surveys currently available, and the surveys with detailed chemical abundance information have been proven especially crucial. Yet a plethora of questions remain open for the next decade. Fortunately, we already know we will have many

of the necessary tools to answer them. There are very exciting times ahead of us in the field of Galactic archaeology.

SUMMARY POINTS

1. The evidence discussed in this review supports the view that a milestone in Galactic history has been unveiled, namely, the last big merger experienced by the Milky Way 10 Gyr ago. The merged galaxy, known as Gaia-Enceladus, appears to be responsible for a large fraction of the inner stellar halo.
2. A disk component was present at the time of merger with Gaia-Enceladus, which is possibly related to the metal-weak thick disk. This disk component was significantly perturbed as a consequence of the merger, and it is currently responsible for roughly 50% of the stars with halo-like kinematics near the Sun—it seems to constitute what has been known as the in-situ halo. There is also some evidence that the merger with Gaia-Enceladus triggered significant star formation in the thick disk, and it seems plausible that the merger was responsible for the formation of a large fraction of the thick disk's stars.
3. These results are consistent with the predictions of the ΛCDM model to first order. Objects in cosmological simulations with similar merger histories have been identified and are providing new insights into the evolution of the various Galactic components, and into how their histories may be interlinked.
4. Several other kinematic substructures have been identified among nearby stars and are likely associated with past accretion events. The Helmi streams ($\sim 10^8\,M_\odot$), (bonsai) Sequoia ($\sim 10^7\,M_\odot$), and Thamnos ($\sim 5 \times 10^6\,M_\odot$), together with Gaia-Enceladus ($\sim 10^9\,M_\odot$) and Sagittarius ($\sim 5 \times 10^8\,M_\odot$), appear to be the largest building blocks of the halo of our Galaxy, although it is not always clear how and if they are related to each other. For some of these (the Helmi streams, Gaia-Enceladus, and Sagittarius) it has been possible to derive (sketchy) star formation histories, and their chemical characterization has only just begun via chemical labeling. The biggest current limitation is the availability of large samples of stars with detailed chemical abundance information, but when available, this information turns out to be crucial.
5. When large samples of stars with detailed chemical abundance information become available, it will be possible to do true Galactic archaeology and establish the properties of the galaxies (star formation and chemical enrichment histories, mass, size) before they were accreted—to really explore the high-redshift universe from our own backyard. It should also be possible to carry out a similar exercise for the thick disk, or the proto-disk, which we know was present 10 Gyr ago (at $z \sim 1.8$) and seems to have been traced back to metallicities [Fe/H] $\lesssim -4$ (Sestito et al. 2019). Establishing the properties of this disk (structure, star formation) will allow us to make a direct link to high-redshift disks currently observed in situ.
6. Most of the above-mentioned building blocks were identified using full phase-space information of stars in the Solar vicinity. At larger distances (beyond 20 kpc from the Galactic center, 10 kpc from the Sun), little is known about the kinematics and chemistry of the stars, but several large substructures have been known for a while thanks to wide-field photometric surveys. These include Hercules-Aquila and the Virgo overdensity, as well as several others. The relation between these and the so-far

identified building blocks, if any, has not been really pinned down, although we present here a way forward using orbital integrations. With *Gaia* DR3 and subsequent releases (DR4 and beyond, since the mission has been extended over the nominal lifetime for at least 2 years), and in combination with spectroscopic surveys, it should be possible to address this and many more questions.

7. In the direction toward the Galactic center, similarly little is known, yet this is where the halo reaches its highest density. Merger debris from another massive building block might well be present [as suggested by the analysis of the age-metallicity relations and dynamics of globular clusters by Kruijssen et al. (2019) and Massari et al. (2019), and which could be a "kraken"-like object]. It is not clear at this point if *Gaia* can answer this, but an astrometric mission in the near infrared (see, e.g., Gouda 2015, Hobbs et al. 2019) could perhaps address this open question.
8. There is more to be gained from the analysis of substructures in the vicinity of the Sun. For example, some may well be due to internal mechanisms (such as the Galactic bar or non-integrability of a generic Galactic potential) or even reveal the response of the Galaxy to an accretion event. For the analysis of the substructures, as well as to address the issues mentioned in previous items, more detailed modeling is needed, also from a dynamical perspective, and preferably through zoom-in cosmological simulations, which now could model systems that, at least in terms of their merger history, would be much more representative of the Milky Way.

FUTURE ISSUES

1. It would be challenging but extremely interesting to identify accretion events that took place even before the merger with Gaia-Enceladus 10 Gyr ago.
2. The characterization (in terms of dynamical, chemical, and star formation history) of the disk present at the time of the merger with Gaia-Enceladus should be pursued. An important link remains to be made between the disks observed in situ in high-z observational studies and that revealed in the Milky Way.
3. Zoom-in cosmological simulations of systems with a merger history and dynamics similar to those suggested by recent data would be particularly useful for understanding Galactic history and the links between the Galaxy's various components and detailed properties. Such simulations would also allow to make robust predictions for direct-detection dark matter experiments.
4. There is an ever-increasing need for large, high-resolution spectroscopic surveys of relatively faint stars ($G \gtrsim 16$) to supplement the dynamical information that is becoming available thanks to the *Gaia* mission. Determination of precise ages for such a sample of stars would be highly valuable and useful to date various events in Galactic history, particularly at early times.

DISCLOSURE STATEMENT

The author is not aware of any affiliations, memberships, funding, or financial holdings that might be perceived as affecting the objectivity of this review.

ACKNOWLEDGMENTS

Very many thanks to all my collaborators throughout the years. I especially acknowledge all my former bachelor, MS, and PhD students, as well as my former postdocs, who contributed directly or indirectly to this review with their ideas, enthusiasm, and dedication. I am particularly indebted to Helmer Koppelman, Davide Massari, Maarten Breddels, and Jovan Veljanoski for the incredible ride since *Gaia* DR1, in the search for truth and the Milky Way's history. The *Gaia* consortium (DPAC), and especially Anthony Brown, are particularly thanked for their fantastic work and very friendly working atmosphere. I am also grateful to my PhD advisors, Simon White and Tim de Zeeuw, for their mentorship throughout my career. Several colleagues, including Helmer Koppelman, Tadafumi Matsuno, Eline Tolstoy, and Tim de Zeeuw, read early drafts and contributed with comments that helped improve this review. I am also grateful to the editor, Joss Bland-Hawthorn, for the open and constructive remarks, and to Eduardo Balbinot and Helmer Koppelman, who helped with several of the figures included in this review. My son Manuel is especially thanked for his patience and continuous encouragement. Data from the European Space Agency mission *Gaia* (**http://www.cosmos.esa.int/gaia**), processed by the *Gaia* DPAC (see **http://www.cosmos.esa.int/web/gaia/dpac/consortium**), are used in this article. Funding for DPAC has been provided by national institutions, in particular, the institutions participating in the *Gaia* Multilateral Agreement. Data from the APOGEE survey, which is part of SDSS-IV, are also used. SDSS-IV is managed by the Astrophysical Research Consortium for the Participating Institutions of the SDSS Collaboration. I also gratefully acknowledge financial support from NOVA, NWO through a Vici grant, and more recently the Spinoza prize.

LITERATURE CITED

Abadi MG, Navarro JF, Steinmetz M, Eke VR. 2003. *Ap. J.* 597:21–34
Abbott TMC, Abdalla FB, Allam S, et al. 2018. *Ap. J. Suppl.* 239:18
Adibekyan VZ, Santos NC, Sousa SG, Israelian G. 2011. *Astron. Astrophys.* 535:L11
Alves-Brito A, Meléndez J, Asplund M, Ramírez I, Yong D. 2010. *Astron. Astrophys.* 513:A35
Amorisco NC. 2017. *MNRAS* 464:2882–95
Antoja T, Helmi A, Romero-Gómez M, et al. 2018. *Nature* 561:360–62
Antoja T, Monari G, Helmi A, et al. 2015. *Ap. J. Lett.* 800:L32
Aoki W, Beers TC, Christlieb N, et al. 2007. *Ap. J.* 655:492–521
Arenou F, Luri X, Babusiaux C, et al. 2018. *Astron. Astrophys.* 616:A17
Arlandini C, Käppeler F, Wisshak K, et al. 1999. *Ap. J.* 525:886–900
Auvergne M, Bodin P, Boisnard L, et al. 2009. *Astron. Astrophys.* 506:411–24
Bahcall JN, Soneira RM. 1984. *Ap. J. Suppl.* 55:67–99
Banerjee A, Jog CJ. 2011. *Ap. J. Lett.* 732:L8
Barbá RH, Minniti D, Geisler D, et al. 2019. *Ap. J. Lett.* 870:L24
Barbuy B, Chiappini C, Gerhard O. 2018. *Annu. Rev. Astron. Astrophys.* 56:223–76
Barnes JE. 1992. *Ap. J.* 393:484–507
Battistini C, Bensby T. 2016. *Astron. Astrophys.* 586:A49
Baugh CM, Cole S, Frenk CS, Lacey CG. 1998. *Ap. J.* 498:504–21
Beers TC, Carollo D, Ivezić Ž, et al. 2012. *Ap. J.* 746:34
Beers TC, Chiba M, Yoshii Y, et al. 2000. *Astron. J.* 119:2866–81
Beers TC, Drilling JS, Rossi S, et al. 2002. *Astron. J.* 124:931–48
Bekki K, Freeman KC. 2003. *MNRAS* 346:L11–15
Belokurov V. 2013. *New Astron. Rev.* 57:100–21
Belokurov V, Erkal D, Evans NW, Koposov SE, Deason AJ. 2018. *MNRAS* 478:611–19
Belokurov V, Evans NW, Bell EF, et al. 2007. *Ap. J. Lett.* 657:L89–92

Belokurov V, Sanders JL, Fattahi A, et al. 2020. *MNRAS* 494:3880–98
Belokurov V, Zucker DB, Evans NW, et al. 2006. *Ap. J. Lett.* 642:L137–40
Bensby T, Feltzing S, Lundström I. 2003. *Astron. Astrophys.* 410:527–51
Bensby T, Feltzing S, Oey MS. 2014. *Astron. Astrophys.* 562:A71
Bernard EJ, Ferguson AMN, Schlafly EF, et al. 2016. *MNRAS* 463:1759–68
Bica E, Bonatto C, Barbuy B, Ortolani S. 2006. *Astron. Astrophys.* 450:105–15
Bignone LA, Helmi A, Tissera PB. 2019. *Ap. J. Lett.* 883:L5
Binney J, Tremaine S. 2008. *Galactic Dynamics*. Princeton, NJ: Princeton Univ. Press. 2nd ed.
Bird JC, Kazantzidis S, Weinberg DH, et al. 2013. *Ap. J.* 773:43
Bisterzo S, Gallino R, Straniero O, Cristallo S, Käppeler F. 2010. *MNRAS* 404:1529–44
Bland-Hawthorn J. 1999. *Nature* 400:220–21
Bland-Hawthorn J, Freeman K. 2000. *Science* 287:79
Bland-Hawthorn J, Gerhard O. 2016. *Annu. Rev. Astron. Astrophys.* 54:529–96
Bland-Hawthorn J, Sharma S, Tepper-Garcia T, Binney J, Freeman KC, et al. 2019. *MNRAS* 486:1167–91
Bonaca A, Conroy C, Wetzel A, Hopkins PF, Kereš D. 2017. *Ap. J.* 845:101
Bonaca A, Hogg DW, Price-Whelan AM, Conroy C. 2019. *Ap. J.* 880:38
Borsato NW, Martell SL, Simpson JD. 2020. *MNRAS* 492:1370–84
Bos R. 2019. *Characterization of a simulated minor merger resembling Gaia-Enceladus*. BSc Thesis, Astron. Dep., Univ. Groningen, Neth.
Bournaud F, Elmegreen BG, Elmegreen DM. 2007. *Ap. J.* 670:237–48
Bournaud F, Elmegreen BG, Martig M. 2009. *Ap. J.* 707:L1–5
Bovy J. 2015. *Ap. J. Suppl.* 216:29
Bovy J, Erkal D, Sanders JL. 2017. *MNRAS* 466:628–68
Bovy J, Rix HW, Hogg DW. 2012. *Ap. J.* 751:131
Bowden A, Evans NW, Williams AA. 2016. *MNRAS* 460:329–37
Brauer K, Ji AP, Frebel A, et al. 2019. *Ap. J.* 871:247
Brinchmann J, Charlot S, White SDM, et al. 2004. *MNRAS* 351:1151–79
Brook CB, Kawata D, Gibson BK, Flynn C. 2003. *Ap. J. Lett.* 585:L125–29
Brook CB, Kawata D, Gibson BK, Freeman KC. 2004. *Ap. J.* 612:894–99
Buckley MR, Hogg DW, Price-Whelan AM. 2019. arXiv:1907.00987 [astro-ph.GA]
Buist HJT, Helmi A. 2015. *Astron. Astrophys.* 584:A120
Buist HJT, Helmi A. 2017. *Astron. Astrophys.* 601:A37
Burton WB. 1988. *Trans. Int. Astron. Union Ser. A* 20A:377–421
Busso M, Gallino R, Wasserburg GJ. 1999. *Annu. Rev. Astron. Astrophys.* 37:239–309
Cantat-Gaudin T, Jordi C, Vallenari A, Bragaglia A, Balaguer-Núñez, et al. 2018. *Astron. Astrophys.* 618:A93
Carney BW, Laird JB, Latham DW, Aguilar LA. 1996. *Astron. J.* 112:668
Carollo D, Beers TC, Chiba M, Norris JE, Freeman KC, et al. 2010. *Ap. J.* 712:692–727
Carollo D, Beers TC, Lee YS, et al. 2007. *Nature* 450:1020–25
Carollo D, Freeman K, Beers TC, et al. 2014. *Ap. J.* 788:180
Carollo D, Tissera PB, Beers TC, et al. 2018. *Ap. J. Lett.* 859:L7
Carretta E, Bragaglia A, Gratton RG, et al. 2009. *Astron. Astrophys.* 505:117–38
Casey AR, Hawkins K, Hogg DW, et al. 2017. *Ap. J.* 840:59
Chambers KC, Magnier EA, Metcalfe N, et al. 2016. arXiv:1612.05560 [astro-ph.IM]
Chaplin WJ, Basu S, Huber D, et al. 2014. *Ap. J. Suppl.* 210:1
Chaplin WJ, Miglio A. 2013. *Annu. Rev. Astron. Astrophys.* 51:353–92
Cheng JY, Rockosi CM, Morrison HL, et al. 2012. *Ap. J.* 752:51
Chiappini C, Matteucci F, Gratton R. 1997. *Ap. J.* 477:765–80
Chiba M, Beers TC. 2000. *Astron. J.* 119:2843–65
Chiba M, Yoshii Y. 1998. *Astron. J.* 115:168–92
Christlieb N, Battistini C, Bonifacio P, et al. 2019. *Messenger* 175:26–29
Conroy C, Bonaca A, Cargile P, et al. 2020. *Ap. J.* 883:107
Conti PS, Greenstein JL, Spinrad H, Wallerstein G, Vardya MS. 1967. *Ap. J.* 148:105–27

Cooper AP, Cole S, Frenk CS, et al. 2010. *MNRAS* 406:744–66
Cowan JJ, Sneden C, Lawler JE, et al. 2019. arXiv:1901.01410 [astro-ph.HE]
Dalton G, Trager S, Abrams DC, et al. 2016. In *Ground-based and Airborne Instrumentation for Astronomy VI*, Vol. 9908, ed. CJ Evans, L Simard, H Takami. Bellingham, WA: SPIE
Das P, Hawkins K, Jofre P. 2020. *MNRAS* 493:5195–207
de Boer TJL, Belokurov V, Koposov SE, et al. 2018. *MNRAS* 477:1893–902
de Jong JTA, Yanny B, Rix HW, et al. 2010. *Ap. J.* 714:663–74
de Jong RS, Agertz O, Berbel AA, et al. 2019. *Messenger* 175:3–11
De Silva GM, Freeman KC, Bland-Hawthorn J, et al. 2015. *MNRAS* 449:2604–17
De Silva GM, Sneden C, Paulson DB, et al. 2006. *Astron. J.* 131:455–60
de Zeeuw T, Norris J. 1999. *Publ. Astron. Soc. Pac.* 111:653–55
Deason AJ, Belokurov V, Evans NW. 2011. *MNRAS* 416:2903–15
Deason AJ, Belokurov V, Evans NW, Johnston KV. 2013. *Ap. J.* 763:113
Deason AJ, Belokurov V, Koposov SE, et al. 2017. *MNRAS* 470:1259–73
Deason AJ, Belokurov V, Koposov SE, Lancaster L. 2018. *Ap. J. Lett.* 862:L1
Deason AJ, Belokurov V, Sanders JL. 2019. *MNRAS* 490:3426–39
Dehnen W. 2000. *Astron. J.* 119:800–12
Dekel A, Birnboim Y, Engel G, et al. 2009. *Nature* 457:451–54
Deng LC, Newberg HJ, Liu C, et al. 2012. *Res. Astron. Astrophys.* 12:735–54
Di Matteo P, Gómez A, Haywood M, et al. 2015. *Astron. Astrophys.* 577:A1
Di Matteo P, Haywood M, Lehnert MD, et al. 2019. *Astron. Astrophys.* 632:A4
Di Matteo P, Lehnert MD, Qu Y, van Driel W. 2011. *Astron. Astrophys.* 525:L3
Diemand J, Madau P, Moore B. 2005. *MNRAS* 364:367–83
Dierickx M, Klement R, Rix HW, Liu C. 2010. *Ap. J. Lett.* 725:L186–90
Dierickx MIP, Loeb A. 2017. *Ap. J.* 836:92
Dinescu DI. 2002. In *Omega Centauri, A Unique Window into Astrophysics*, ed. F van Leeuwen, JD Hughes, G Piotto, pp. 143–54. San Francisco: Astron. Soc. Pac.
Donlon T II, Newberg HJ, Weiss J, Amy P, Thompson J. 2019. *Ap. J.* 886:76
Eadie G, Jurić M. 2019. *Ap. J.* 875:159
Eggen OJ, Lynden-Bell D, Sandage AR. 1962. *Ap. J.* 136:748–66
El-Badry K, Bland-Hawthorn J, Wetzel A, et al. 2018. *MNRAS* 480:652–68
Elbaz D, Dickinson M, Hwang HS, et al. 2011. *Astron. Astrophys.* 533:A119
Eneev TM, Kozlov NN, Sunyaev RA. 1973. *Astron. Astrophys.* 22:41
Erkal D, Belokurov V, Laporte CFP, et al. 2019. *MNRAS* 487:2685–700
Fardal MA, van der Marel RP, Law DR, et al. 2019. *MNRAS* 483:4724–41
Fattahi A, Belokurov V, Deason AJ, et al. 2019. *MNRAS* 484:4471–83
Fernández-Alvar E, Carigi L, Schuster WJ, et al. 2018. *Ap. J.* 852:50
Fernández-Trincado JG, Beers TC, Placco VM, et al. 2019. *Ap. J. Lett.* 886:L8
Font AS, Johnston KV, Bullock JS, Robertson BE. 2006. *Ap. J.* 646:886–98
Fragkoudi F, Di Matteo P, Haywood M, et al. 2018. *Astron. Astrophys.* 616:A180
Frebel A, Norris JE. 2015. *Annu. Rev. Astron. Astrophys.* 53:631–88
Freeman K, Bland-Hawthorn J. 2002. *Annu. Rev. Astron. Astrophys.* 40:487–537
Frenk CS, White SDM. 2012. *Ann. Phys.* 524:507–34
Fuhrmann K. 2011. *MNRAS* 414:2893–922
Gaia Collab., Babusiaux C, van Leeuwen F, et al. 2018a. *Astron. Astrophys.* 616:A10
Gaia Collab., Brown AGA, Vallenari A, et al. 2016. *Astron. Astrophys.* 595:A2
Gaia Collab., Brown AGA, Vallenari A, et al. 2018b. *Astron. Astrophys.* 616:A1
Gaia Collab., Helmi A, van Leeuwen F, et al. 2018c. *Astron. Astrophys.* 616:A12
Gaia Collab., Katz D, Antoja T, et al. 2018d. *Astron. Astrophys.* 616:A11
Gallart C, Bernard EJ, Brook CB, et al. 2019. *Nat. Astron.* 3:932–39
Gerin M, Combes F, Athanassoula E. 1990. *Astron. Astrophys.* 230:37–54

Gibson BK, Axelrod RS, Putman ME. 1999. *The Third Stromlo Symposium: The Galactic Halo*. San Francisco: Astron. Soc. Pac.
Gilliland RL, Brown TM, Christensen-Dalsgaard J, et al. 2010. *Publ. Astron. Soc. Pac.* 122:131
Gilmore G, Reid N. 1983. *MNRAS* 202:1025–47
Gilmore G, Wyse RFG, Jones JB. 1995. *Astron. J.* 109:1095–1111
Gilmore G, Wyse RFG, Kuijken K. 1989. *Annu. Rev. Astron. Astrophys.* 27:555–627
Gilmore G, Wyse RFG, Norris JE. 2002. *Ap. J. Lett.* 574:L39–42
Gómez FA, Helmi A. 2010. *MNRAS* 401:2285–98
Gómez FA, Helmi A, Cooper AP, et al. 2013. *MNRAS* 436:3602–13
Gómez FA, Minchev I, Villalobos Á, O'Shea BW, Williams MEK. 2012. *MNRAS* 419:2163–72
Gouda N. 2015. *IAU Gen. Assembl.* 29:2247720
Gould A. 2003. *Ap. J. Lett.* 592:L63–L66
Grand RJJ, Gómez FA, Marinacci F, et al. 2017. *MNRAS* 467:179–207
Grand RJJ, Helly J, Fattahi A, et al. 2018. *MNRAS* 481:1726–43
Gratton R, Bragaglia A, Carretta E, et al. 2019. *Astron. Astrophys. Rev.* 27:8
Gravity Collab., Abuter R, Amorim A, et al. 2019. *Astron. Astrophys.* 625:L10
Grillmair CJ. 2011. *Ap. J.* 738:98
Grillmair CJ, Carlin JL. 2016. In *Tidal Streams in the Local Group and Beyond*, ed. HJ Newberg, JL Carlin, pp. 87–112. New York: Springer
Hagen JHJ. 2020. *Galactic dynamics in the era of Gaia*. PhD Thesis, Univ. Groningen, Neth.
Hawkins K, Jofré P, Gilmore G, Masseron T. 2014. *MNRAS* 445:2575–88
Hayden MR, Bovy J, Holtzman JA, et al. 2015. *Ap. J.* 808:132
Hayes CR, Majewski SR, Shetrone M, et al. 2018. *Ap. J.* 852:49
Haynes CJ, Kobayashi C. 2019. *MNRAS* 483:5123–34
Haywood M, Di Matteo P, Lehnert MD, Katz D, Gómez A. 2013. *Astron. Astrophys.* 560:A109
Haywood M, Di Matteo P, Lehnert MD, et al. 2018. *Ap. J.* 863:113
Haywood M, Di Matteo P, Snaith O, Lehnert MD. 2015. *Astron. Astrophys.* 579:A5
Helmi A. 2004. *Ap. J. Lett.* 610:L97–100
Helmi A. 2008. *Astron. Astrophys. Rev.* 15:145–88
Helmi A, Babusiaux C, Koppelman HH, et al. 2018. *Nature* 563:85–88
Helmi A, de Zeeuw PT. 2000. *MNRAS* 319:657–65
Helmi A, Irwin M, Deason A, et al. 2019. *Messenger* 175:23–25
Helmi A, Navarro JF, Nordström B, et al. 2006. *MNRAS* 365:1309–23
Helmi A, Veljanoski J, Breddels MA, Tian H, Sales LV. 2017. *Astron. Astrophys.* 598:A58
Helmi A, White SDM. 1999. *MNRAS* 307:495–517
Helmi A, White SDM, de Zeeuw PT, Zhao H. 1999. *Nature* 402:53–55
Helmi A, White SDM, Springel V. 2002. *Phys. Rev. D* 66:063502
Helmi A, White SDM, Springel V. 2003. *MNRAS* 339:834–48
Helmi A, Williams M, Freeman KC, Bland-Hawthorn J, De Silva G. 2014. *Ap. J.* 791:135
Hendel D, Johnston KV. 2015. *MNRAS* 454:2472–85
Hobbs D, Brown A, Høg E, et al. 2019. arXiv:1907.12535 [astro-ph.IM]
Homma H, Murayama T, Kobayashi MAR, Taniguchi Y. 2015. *Ap. J.* 799:230
Hopkins PF, Kerěs D, Oñorbe J, et al. 2014. *MNRAS* 445:581–603
Ibata R, Lewis GF, Irwin M, Totten E, Quinn T. 2001. *Ap. J.* 551:294–311
Ibata R, Lewis GF, Martin NF, Bellazzini M, Correnti M. 2013. *Ap. J. Lett.* 765:L15
Ibata RA, Bellazzini M, Malhan K, Martin N, Bianchini P. 2019. *Nat. Astron.* 3:667–72
Ibata RA, Gilmore G, Irwin MJ. 1994. *Nature* 370:194–96
Ibata RA, Malhan K, Martin NF. 2019. *Ap. J.* 872:152
Iorio G, Belokurov V. 2019. *MNRAS* 482:3868–79
Ishigaki MN. 2019. In *Star Clusters: From the Milky Way to the Early Universe*, ed. A Bragaglia, M Davies, A Sills, E Vesperini, pp. 24–33. Cambridge, UK: Cambridge Univ. Press
Ivezić Ž, Goldston J, Finlator K, et al. 2000. *Astron. J.* 120:963–77

Ivezić Ž, Kahn SM, Tyson JA, et al. 2019. *Ap. J.* 873:111
Jean-Baptiste I, Di Matteo P, Haywood M, et al. 2017. *Astron. Astrophys.* 604:A106
Ji AP, Frebel A, Chiti A, Simon JD. 2016. *Nature* 531:610–13
Johnston KV. 1998. *Ap. J.* 495:297–308
Johnston KV. 2016. In *Tidal Streams in the Local Group and Beyond*, ed. HJ Newberg, JL Carlin, pp. 141–67. New York: Springer
Johnston KV, Hernquist L, Bolte M. 1996. *Astrophys. J.* 465:278
Johnston KV, Law DR, Majewski SR. 2005. *Ap. J.* 619:800–6
Jurić M, Ivezić Ž, Brooks A, et al. 2008. *Ap. J.* 673:864–914
Kafle PR, Sharma S, Lewis GF, Bland-Hawthorn J. 2014. *Ap. J.* 794:59
Käppeler F, Gallino R, Bisterzo S, Aoki W. 2011. *Rev. Mod. Phys.* 83:157–94
Kauffmann G, White SDM, Guiderdoni B. 1993. *MNRAS* 264:201–18
Kawata D, Chiappini C. 2016. *Astron. Nachr.* 337:976
Kepley AA, Morrison HL, Helmi A, et al. 2007. *Astron. J.* 134:1579–95
Khanna S, Sharma S, Tepper-Garcia T, et al. 2019. *MNRAS* 489:4962–79
Kilic M, Munn JA, Harris HC, et al. 2017. *Ap. J.* 837:162
Kinman TD, Cacciari C, Bragaglia A, Buzzoni A, Spagna A. 2007. *MNRAS* 375:1381–98
Klement RJ. 2010. *Astron. Astrophys. Rev.* 18:567–94
Klypin A, Kravtsov AV, Valenzuela O, Prada F. 1999. *Ap. J.* 522:82–92
Kollmeier J, Fuller J, Gaensicke B, et al. 2019. *Bull. Am. Astron. Soc.* 51:503
Koposov SE, Belokurov V, Li TS, et al. 2019. *MNRAS* 485:4726–42
Koposov SE, Rix HW, Hogg DW. 2010. *Ap. J.* 712:260–73
Koppelman H, Helmi A, Veljanoski J. 2018. *Ap. J. Lett.* 860:L11
Koppelman HH, Helmi A, Massari D, Price-Whelan AM, Starkenburg TK. 2019a. *Astron. Astrophys.* 631:L9
Koppelman HH, Helmi A, Massari D, Roelenga S, Bastian U. 2019b. *Astron. Astrophys.* 625:A5
Kordopatis G, Hill V, Irwin M, et al. 2013. *Astron. Astrophys.* 555:A12
Kruijssen JMD, Pfeffer JL, Reina-Campos M, Crain RA, Bastian N. 2019. *MNRAS* 486:3180–202
Kunder A, Kordopatis G, Steinmetz M, et al. 2017. *Astron. J.* 153:75
Lanfranchi GA, Matteucci F. 2010. *Astron. Astrophys.* 512:A85
Laporte CFP, Gómez FA, Besla G, Johnston KV, Garavito-Camargo N. 2018a. *MNRAS* 473:1218–30
Laporte CFP, Johnston KV, Gómez FA, Garavito-Camargo N, Besla G. 2018b. *MNRAS* 481:286–306
Laporte CFP, Minchev I, Johnston KV, Gómez FA. 2019. *MNRAS* 485:3134–52
Larsen JA, Cabanela JE, Humphreys RM. 2011. *Astron. J.* 141:130
Larsen JA, Humphreys RM. 1996. *Ap. J. Lett.* 468:L99–102
Law DR, Majewski SR. 2010. *Ap. J.* 718:1128–50
Lee YS, Beers TC, Kim YK. 2019. *Ap. J.* 885:102
Lehnert MD, Di Matteo P, Haywood M, Snaith ON. 2014. *Ap. J. Lett.* 789:L30
Levi M, Allen LE, Raichoor A, et al. 2019. *Bull. Am. Astron. Soc.* 51:57
Liang XL, Zhao JK, Oswalt TD, et al. 2017. *Ap. J.* 844:152
Licquia TC, Newman JA. 2015. *Ap. J.* 806:96
Lindegren L, Hernández J, Bombrun A, et al. 2018. *Astron. Astrophys.* 616:A2
Lindegren L, Lammers U, Bastian U, et al. 2016. *Astron. Astrophys.* 595:A4
Liu C, van de Ven G. 2012. *MNRAS* 425:2144–56
Lowing B, Wang W, Cooper A, et al. 2015. *MNRAS* 446:2274–90
Mackereth JT, Bovy J. 2020. *MNRAS* 492:3631–46
Mackereth JT, Schiavon RP, Pfeffer J, et al. 2019. *MNRAS* 482:3426–42
Majewski SR, Munn JA, Hawley SL. 1994. *Ap. J. Lett.* 427:L37
Majewski SR, Munn JA, Hawley SL. 1996. *Ap. J. Lett.* 459:L73
Majewski SR, Schiavon RP, Frinchaboy PM, et al. 2017. *Astron. J.* 154:94
Malhan K, Ibata RA. 2018. *MNRAS* 477:4063–76
Malhan K, Ibata RA, Carlberg RG, Valluri M, Freese K. 2019. *Ap. J.* 881:106
Malhan K, Ibata RA, Martin NF. 2018. *MNRAS* 481:3442–55

Maoz D, Mannucci F, Nelemans G. 2014. *Annu. Rev. Astron. Astrophys.* 52:107–70
Martell SL, Shetrone MD, Lucatello S, et al. 2016. *Ap. J.* 825:146
Martinez-Valpuesta I, Gerhard O. 2013. *Ap. J.* 766:L3
Massari D, Koppelman HH, Helmi A. 2019. *Astron. Astrophys.* 630:L4
Mateu C, Read JI, Kawata D. 2018. *MNRAS* 474:4112–29
Matsuno T, Aoki W, Suda T. 2019. *Ap. J. Lett.* 874:L35
Matteucci F, Recchi S. 2001. *Ap. J.* 558:351–58
Matteucci F, Spitoni E, Rojas-Arriagada A, Schultheis M. 2018. Presentation at The Galactic Bulge at the Crossroads (GBX2018), Pucón, Chile, Dec. 10–14
McMillan PJ. 2018. *Res. Notes Am. Astron. Soc.* 2:51
McMillan PJ, Binney JJ. 2008. *MNRAS* 390:429–37
McWilliam A. 1997. *Annu. Rev. Astron. Astrophys.* 35:503–56
Meza A, Navarro JF, Abadi MG, Steinmetz M. 2005. *MNRAS* 359:93–103
Michel E, Baglin A, Auvergne M, et al. 2008. *Science* 322:558
Miglio A, Chiappini C, Morel T, et al. 2013. *MNRAS* 429:423–28
Minchev I, Famaey B, Quillen AC, et al. 2012. *Astron. Astrophys.* 548:A127
Minchev I, Martig M, Streich D, et al. 2015. *Ap. J. Lett.* 804:L9
Minchev I, Steinmetz M, Chiappini C, et al. 2017. *Ap. J.* 834:27
Mints A, Hekker S. 2018. *Astron. Astrophys.* 618:A54
Mo H, van den Bosch FC, White S. 2010. *Galaxy Formation and Evolution*. Cambridge, UK: Cambridge Univ. Press
Mo HJ, Mao S, White SDM. 1998. *MNRAS* 295:319–36
Moore B, Ghigna S, Governato F, et al. 1999. *Ap. J. Lett.* 524:L19–22
Morrison HL. 1993. *Astron. J.* 105:539
Morrison HL, Flynn C, Freeman KC. 1990. *Astron. J.* 100:1191
Morrison HL, Helmi A, Sun J, et al. 2009. *Ap. J.* 694:130–43
Myeong GC, Evans NW, Belokurov V, Amorisco NC, Koposov SE. 2018a. *MNRAS* 475:1537–48
Myeong GC, Evans NW, Belokurov V, Sanders JL, Koposov SE. 2018b. *Ap. J. Lett.* 863:L28
Myeong GC, Vasiliev E, Iorio G, Evans NW, Belokurov V. 2019. *MNRAS* 488:1235–47
Naiman JP, Pillepich A, Springel V, et al. 2018. *MNRAS* 477:1206–24
Navarrete C, Chanamé J, Ramírez I, et al. 2015. *Ap. J.* 808:103
Necib L, Lisanti M, Garrison-Kimmel S, et al. 2019a. *Ap. J.* 883:27
Necib L, Ostdiek B, Lisanti M, et al. 2019b. arXiv:1907.07681 [astro-ph.GA]
Nelson D, Springel V, Pillepich A, et al. 2019. *Comput. Astrophys. Cosmol.* 6:2
Ness M, Bird J, Johnson J, et al. 2019. *Bull. Am. Astron. Soc.* 51:238
Ness M, Freeman K, Athanassoula E, et al. 2013. *MNRAS* 430:836–57
Newberg HJ, Carlin JL, eds. 2016. *Tidal Streams in the Local Group and Beyond: Observations and Implications*. New York: Springer
Newberg HJ, Yanny B, Rockosi C, et al. 2002. *Ap. J.* 569:245–74
Nissen PE, Schuster WJ. 1997. *Astron. Astrophys.* 326:751–62
Nissen PE, Schuster WJ. 2010. *Astron. Astrophys.* 511:L10
Nissen PE, Schuster WJ. 2011. *Astron. Astrophys.* 530:A15
Nordström B, Mayor M, Andersen J, et al. 2004. *Astron. Astrophys.* 418:989–1019
Norris J, Bessell MS, Pickles AJ. 1985. *Ap. J. Suppl.* 58:463–92
Norris JE. 1994. *Ap. J.* 431:645
O'Hare CAJ, Evans NW, McCabe C, Myeong G, Belokurov V. 2020. *Phys. Rev. D* 101:023006
Pasquini L, Delabre B, Ellis RS, et al. 2018. In *Rediscovering Our Galaxy*, ed. C Chiappini, I Minchev, E Starkenburg, M Valentini, pp. 242–47. Cambridge, UK: Cambridge Univ. Press
Perryman MAC, Lindegren L, Kovalevsky J, et al. 1997. *Astron. Astrophys.* 500:501–4
Pillepich A, Madau P, Mayer L. 2015. *Ap. J.* 799:184
Pillepich A, Nelson D, Springel V, et al. 2019. *MNRAS* 490:3196–233
Planck Collab., Aghanim N, Arnaud M, et al. 2016. *Astron. Astrophys.* 594:A11

Portail M, Wegg C, Gerhard O, Martinez-Valpuesta I. 2015. *MNRAS* 448:713–31
Posti L, Helmi A. 2019. *Astron. Astrophys.* 621:A56
Price-Whelan AM. 2017. *J. Open Source Softw.* 2(18):388
Price-Whelan AM, Bonaca A. 2018. *Ap. J. Lett.* 863:L20
Price-Whelan AM, Johnston KV, Valluri M, et al. 2016. *MNRAS* 455:1079–98
Price-Whelan AM, Sipocz B, Lenz D, et al. 2019. adrn/gala: v1.0. *Software*. **https://zenodo.org/record/2638307#.XsiLOTpKg2w**
Purcell CW, Bullock JS, Kazantzidis S. 2010. *MNRAS* 404:1711–18
Queiroz ABA, Anders F, Santiago BX, et al. 2018. *MNRAS* 476:2556–83
Quinn PJ. 1984. *Ap. J.* 279:596–609
Quinn PJ, Hernquist L, Fullagar DP. 1993. *Astrophys. J.* 403:74–93
Rauer H, Aerts C, Cabrera J, PLATO Team. 2016. *Astron. Nachr.* 337:961
Re Fiorentin P, Lattanzi MG, Spagna A, Curir A. 2015. *Astron. J.* 150:128
Recio-Blanco A, de Laverny P, Kordopatis G, et al. 2014. *Astron. Astrophys.* 567:A5
Richter P. 2017. In *Gas Accretion onto Galaxies*, ed. A Fox, R Davé, pp. 15–48. New York: Springer
Ricker GR, Winn JN, Vanderspek R, et al. 2015. *J. Astron. Telesc. Instrum. Syst.* 1:014003
Robin AC, Reylé C, Fliri J, et al. 2014. *Astron. Astrophys.* 569:A13
Roederer IU, Hattori K, Valluri M. 2018. *Astron. J.* 156:179
Roederer IU, Sneden C, Thompson IB, Preston GW, Shectman SA. 2010. *Ap. J.* 711:573–96
Roman NG. 1950. *Ap. J.* 112:554–59
Roman NG. 2019. *Annu. Rev. Astron. Astrophys.* 57:1–34
Sakari CM, Placco VM, Farrell EM, et al. 2018. *Ap. J.* 868:110
Sales LV, Helmi A, Abadi MG, et al. 2009. *MNRAS* 400:L61–65
Sales LV, Navarro JF, Kallivayalil N, Frenk CS. 2017. *MNRAS* 465:1879–88
Sanders JL, Binney J. 2013. *MNRAS* 433:1813–25
Sanders JL, Binney J. 2016. *MNRAS* 457:2107–21
Sanders JL, Das P. 2018. *MNRAS* 481:4093–110
Sanderson RE, Wetzel A, Loebman S, et al. 2020. *Ap. J. Suppl.* 246:6
Santucci RM, Beers TC, Placco VM, et al. 2015. *Ap. J. Lett.* 813:L16
Schaye J, Crain RA, Bower RG, et al. 2015. *MNRAS* 446:521–54
Schönrich R, Asplund M, Casagrande L. 2011. *MNRAS* 415:3807–23
Schönrich R, Binney J. 2009. *MNRAS* 399:1145–56
Schuster WJ, Moitinho A, Márquez A, Parrao L, Covarrubias E. 2006. *Astron. Astrophys.* 445:939–58
Schuster WJ, Moreno E, Nissen PE, Pichardo B. 2012. *Astron. Astrophys.* 538:A21
Schwarzschild M. 1979. *Ap. J.* 232:236–47
Searle L, Zinn R. 1978. *Ap. J.* 225:357–79
Sesar B, Hernitschek N, Mitrović S, et al. 2017. *Astron. J.* 153:204
Sestito F, Longeard N, Martin NF, et al. 2019. *MNRAS* 484:2166–80
Sheffield AA, Price-Whelan AM, Tzanidakis A, et al. 2018. *Ap. J.* 854:47
Shen J, Rich RM, Kormendy J, et al. 2010. *Ap. J. Lett.* 720:L72–76
Shipp N, Drlica-Wagner A, Balbinot E, et al. 2018. *Ap. J.* 862:114
Simion IT, Belokurov V, Koposov SE. 2019. *MNRAS* 482:921–28
Simpson CM, Gargiulo I, Gómez FA, et al. 2019. *MNRAS* 490:L32–37
Skúladóttir Á, Hansen CJ, Salvadori S, Choplin A. 2019. 631:A171
Smith MC. 2016. In *Tidal Streams in the Local Group and Beyond*, ed. HJ Newberg, JL Carlin, pp. 113–39. New York: Springer
Snaith ON, Haywood M, Di Matteo P, et al. 2014. *Ap. J. Lett.* 781:L31
Sneden C, Cowan JJ, Gallino R. 2008. *Annu. Rev. Astron. Astrophys.* 46:241–88
Sneden C, Lambert DL, Whitaker RW. 1979. *Ap. J.* 234:964–72
Somerville RS, Primack JR. 1999. *MNRAS* 310:1087–110
Spite F, Spite M. 1979. *Messenger* 16:7–8
Springel V, Wang J, Vogelsberger M, et al. 2008. *MNRAS* 391:1685–711

Starkenburg E, Oman KA, Navarro JF, et al. 2017. *MNRAS* 465:2212–24
Stonkutė E, Tautvaišienė G, Nordström B, Ženovienė R. 2012. *Astron. Astrophys.* 541:A157
Stonkutė E, Tautvaišienė G, Nordström B, Ženovienė R. 2013. *Astron. Astrophys.* 555:A6
Suda T, Katsuta Y, Yamada S, et al. 2008. *Publ. Astron. Soc. Jpn.* 60:1159
Tamura N, Takato N, Shimono A, et al. 2016. In *Ground-based and Airborne Instrumentation for Astronomy VI*, Vol. 9908, ed. CJ Evans, L Simard, H Takami. Bellingham, WA: SPIE
Taylor C, Boylan-Kolchin M, Torrey P, Vogelsberger M, Hernquist L. 2016. *MNRAS* 461:3483–93
Tinsley BM. 1980. *Fundam. Cosmic Phys.* 5:287–388
Tissera PB, Scannapieco C, Beers TC, Carollo D. 2013. *MNRAS* 432:3391–400
Tolstoy E, Hill V, Tosi M. 2009. *Annu. Rev. Astron. Astrophys.* 47:371–425
Tononi J, Torres S, García-Berro E, et al. 2019. *Astron. Astrophys.* 628:A52
Toomre A, Toomre J. 1972. *Ap. J.* 178:623–66
Travaglio C, Gallino R, Arnone E, et al. 2004. *Ap. J.* 601:864–84
Tremaine S. 1999. *MNRAS* 307:877–83
Tremonti CA, Heckman TM, Kauffmann G, et al. 2004. *Ap. J.* 613:898–913
Tsujimoto T, Matsuno T, Aoki W, Ishigaki MN, Shigeyama T. 2017. *Ap. J. Lett.* 850:L12
Tumlinson J. 2010. *Ap. J.* 708:1398–418
Turon C, Primas F, Binney J, et al. 2008. *Messenger* 134:46–49
Valentini M, Chiappini C, Davies GR, et al. 2017. *Astron. Astrophys.* 600:A66
van Dokkum PG, Leja J, Nelson EJ, et al. 2013. *Ap. J. Lett.* 771:L35
Vera-Ciro C, Helmi A. 2013. *Ap. J. Lett.* 773:L4
Villalobos Á, Helmi A. 2008. *MNRAS* 391:1806–27
Villalobos Á, Helmi A. 2009. *MNRAS* 399:166–76
Vincenzo F, Spitoni E, Calura F, et al. 2019. *MNRAS* 487:L47–L52
Vivas AK, Zinn R, Abad C, et al. 2004. *Astron. J.* 127:1158–75
Vogelsberger M, White SDM, Helmi A, Springel V. 2008. *MNRAS* 385:236–54
Wang J, Navarro JF, Frenk CS, et al. 2011. *MNRAS* 413:1373–82
Watkins LL, Evans NW, Belokurov V, et al. 2009. *MNRAS* 398:1757–70
Watkins LL, van der Marel RP, Sohn ST, Evans NW. 2019. *Ap. J.* 873:118
Watson D, Hansen CJ, Selsing J, et al. 2019. *Nature* 574:497–500
Wegg C, Gerhard O, Bieth M. 2019. *MNRAS* 485:3296–316
Wegg C, Gerhard O, Portail M. 2015. *MNRAS* 450:4050–69
White SDM, Rees MJ. 1978. *MNRAS* 183:341–58
White SDM, Springel V. 2000. In *The First Stars*, ed. A Weiss, TG Abel, V Hill, pp. 327–35. New York: Springer
Wilson ML, Helmi A, Morrison HL, et al. 2011. *MNRAS* 413:2235–41
Wyse RFG, Gilmore G, Norris JE, et al. 2006. *Ap. J. Lett.* 639:L13–16
Xing QF, Zhao G, Aoki W, et al. 2019. *Nat. Astron.* 3:631–35
Xue XX, Rix HW, Ma Z, et al. 2015. *Ap. J.* 809:144
Yang T, Boruah SS, Afshordi N. 2020. *MNRAS* 493:3061–80
Yanny B, Newberg HJ, Kent S, et al. 2000. *Ap. J.* 540:825–41
York DG, Adelman J, Anderson JE Jr., et al. 2000. *Astron. J.* 120:1579–87
Yuan Z, Myeong GC, Beers TC, et al. 2020. *Ap. J.* 891:39
Zaritsky D, McCabe K, Aravena M, et al. 2016. *Ap. J.* 818:99
Ženovienė R, Tautvaišienė G, Nordström B, Stonkutė E, Barisevičius G. 2015. *Astron. Astrophys.* 576:A113
Zheng Y, Peek JEG, Putman ME, Werk JK. 2019. *Ap. J.* 871:35
Zoccali M. 2019. *Bol. Asoc. Argent. Astron.* 61:137–44
Zolotov A, Willman B, Brooks AM, et al. 2009. *Ap. J.* 702:1058–67